THESIS

SKELETAL MUSCLE DERIVED CD81^{+} EXTRACELLULAR VESICLES AS A POTENTIAL THERAPEUTIC FOR INSULIN RESISTANCE IN ADIPOCYTES

Submitted by

Darby Easterday

Department of Health & Exercise Science

In partial fulfillment of the requirements

For the Degree of Master of Science

Colorado State University

Fort Collins, Colorado

Summer 2025

Master's Committee:

Advisor: Dan Lark

Tom LaRocca
Chris Gentile

ABSTRACT

SKELETAL MUSCLE DERIVED CD81^{+} EXTRACELLULAR VESICLES AS A POTENTIAL THERAPEUTIC FOR INSULIN RESISTANCE IN ADIPOCYTES

Obesity and its related metabolic disorders, including insulin resistance (IR), represent a growing public health crisis, with 50% of the U.S. population projected to have obesity by 2030 and an estimated $173 billion cost to the U.S. healthcare system currently. While skeletal muscle and adipose tissue are central to insulin-stimulated glucose disposal, current therapeutic strategies for IR like exercise, pharmacological agents, and bariatric surgery are limited by adherence, accessibility, and a lack of targeted mechanisms. One emerging area of interest in novel therapeutics is the role of extracellular vesicles (EVs), lipid-bound particles released by all cell types that carry bioactive cargo and influence recipient cell behavior. CD81, a tetraspanin protein highly enriched in EVs, plays a structural role in membrane signaling domains and is increasingly implicated as a mediator of insulin sensitivity and adipose tissue homeostasis. Many studies have shown that CD81-expressing EVs are released from skeletal muscle (SkM) and may be capable of modulating metabolic signaling in distal tissues, like adipose tissue.

The purpose of the present study was to investigate the functional impact of skeletal muscle-derived CD81^{+} EVs on adipocyte insulin signaling (Figure 1). Specifically, these studies aimed to determine whether CD81 physically interacts with insulin signaling

machinery, whether loss of CD81 impairs insulin sensitivity, and whether delivery of CD81 via SkM-derived EVs could restore insulin action in adipocytes. Using 3T3L1 preadipocytes, we demonstrate that CD81 co-immunoprecipitates with phosphorylated Akt (pAkt), suggesting a physical interaction between CD81 and insulin signaling machinery. While silencing CD81 did not significantly impair insulin signaling, a modest trend toward reduced pAkt suggests a potential role. Notably, treatment with SkM-derived $CD81^+$ EVs successfully restored CD81 content in CD81-silenced cells, confirming that CD81 can be delivered to adipocytes via EVs, but failed to significantly enhance insulin-stimulated pAkt signaling.

Taken together, these data provide the first evidence that CD81 physically associates with pAkt in preadipocytes and suggest that $CD81^+$ EVs, isolated by magnetically labelled immunocapture, may modulate membrane protein content without strongly altering downstream signaling under the tested conditions. This work contributes to establishing a framework for exploring skeletal muscle-derived $CD81^+$ EVs as a potential tissue-specific therapy for insulin resistance and metabolic dysfunction.

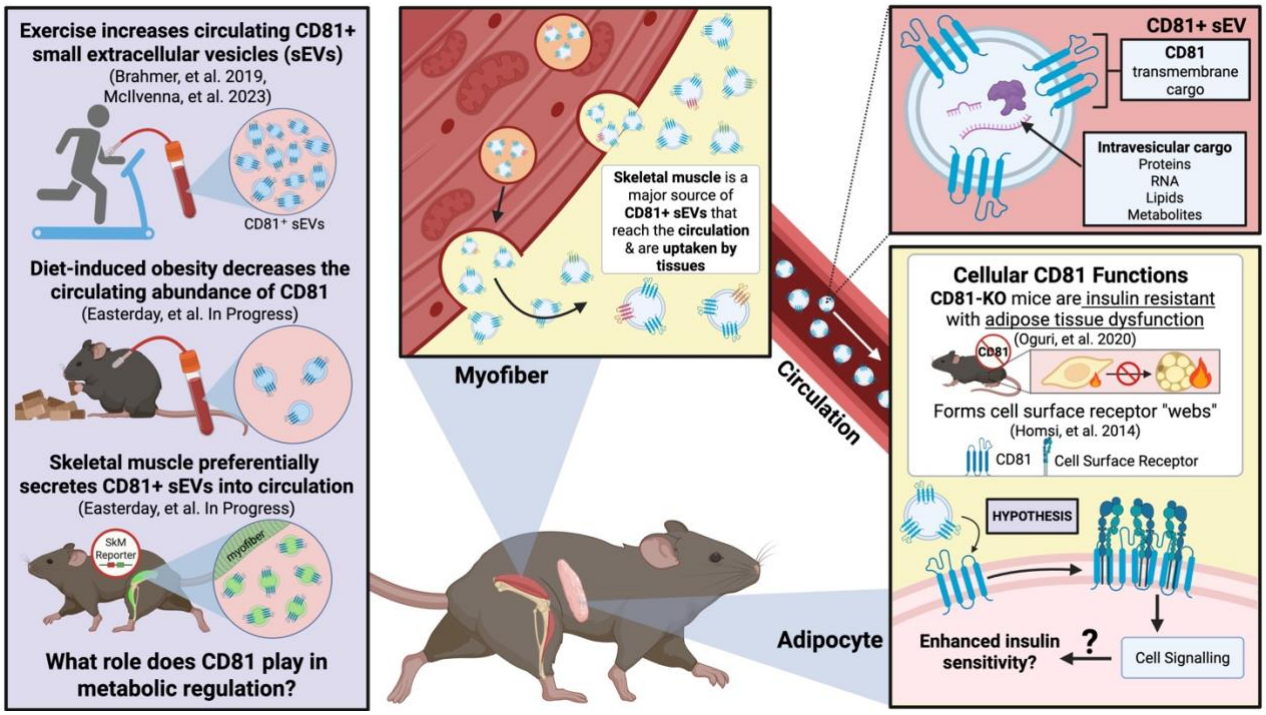

Figure 1: Graphical abstract of “Skeletal muscle-derived CD81+ extracellular vesicles as a potential therapeutic for insulin resistance”

ACKNOWLEDGEMENTS

First and foremost, I would like to thank my mentor, Dr. Dan Lark, for his unwavering support, guidance, and belief in me throughout this project and many others during my time in the Extracellular Regulation of Metabolism Lab. I am deeply grateful for your mentorship and the opportunity to grow under your leadership, one which welcomed my relentless curiosity and fostered confidence in my abilities as a student investigator. Thank you for going above and beyond in supporting my academic career, my future career as a Physician Assistant, and my personal well-being throughout this process. I would also like to thank my thesis committee members, Dr. Tom LaRocca and Dr. Chris Gentile, for their valuable feedback, thoughtful discussions, and encouragement throughout the research and writing process. To the faculty, staff, and fellow graduate students of the Department of Health and Exercise Science- thank you for your support, especially during times when I navigated this journey as the sole graduate researcher in my lab. To shoutout only a few- Dr. Brett Fling, Dr. Dave Thomson, Dr. Matt Hickey, Dr. Maureen Walsh, Dr. Meg Keenan-Smith, Dr. Shelby Osburn, Matt Bomar, Hannah Butterklee, Isaac Bast, Alex Barragan, Jake Dawson, Zoe Willard, and Ellie Shyu, your encouragement, support, and camaraderie meant more than words can describe and was essential to my success in this program. Finally, to my friends and family—thank you for your constant love and encouragement. I am especially grateful to my parents, Dyke and Tess Easterday, my brother, Nash Easterday, my best friends Kristen, Elli, and Sonya, and my partner, Tim. Your support

has been my foundation in school, science, and life. All figures were created in https://BioRender.com.

TABLE OF CONTENTS

CHAPTER 1 - INTRODUCTION

The prevalence of obesity in the U.S. has tripled since the 1960s, now affecting over 40% of adults, with projections nearing 50% by 2030 [1,2]. Clinically defined by a BMI ≥30, obesity reflects excessive adiposity and is strongly linked to chronic conditions like type 2 diabetes (T2DM), cardiovascular disease, metabolic-associated steatotic liver disease (MASLD), neurodegenerative disorders, and cancers[3]Under healthy conditions, insulin-sensitive tissues, like white adipose tissue (WAT) and skeletal muscle (SkM), precisely coordinate macronutrient uptake, storage, and energy balance. The primary insulin signaling cascade is conserved in both of these tissues via the insulin-activated phosphorylation of protein kinase B (Akt)[4]. In WAT, insulin signaling promotes lipid storage, glucose uptake, and adipokine secretion while suppressing lipolysis[5]. In SkM, the primary site of postprandial glucose disposal, insulin signaling promotes glucose uptake, glycogenesis, and protein synthesis[6]. Together, these tissues robustly contribute to regulating systemic metabolic homeostasis.

However, chronic overnutrition and inactivity lead to excessive expansion of WAT depots and the onset of insulin resistance (IR)[7]. In this state, cells fail to initiate the primary phosphorylation events that propagate the insulin signal, impairing glucose uptake and disrupting lipid metabolism. In WAT, IR blunts suppression of lipolysis, resulting in continuous release of free fatty acids (FFAs) into circulation. These FFAs contribute to ectopic lipid accumulation, mitochondrial dysfunction, and systemic inflammation[8]*22. Hyperglycemia, hyperinsulinemia, and chronic FFA exposure create a feedback loop of worsening IR and systemic vascular dysfunction*19. These

pathologies underscore WAT and SkM as critical regulators of metabolic health, and thus, critical targets of therapeutic intervention.

CURRENT THERAPUETIC STRATEGIES AND LIMITATIONS

Existing therapies for IR include exercise/lifestyle modification, GLP-1 receptor agonists, SGLT2 inhibitors, and/or bariatric surgeries. While effective, these interventions have limitations. Pharmacotherapies, like SGLT2 inhibitors and GLP-1 agonists, can cause adverse effects, require injections, or lose efficacy over time[9,10]. Bariatric surgery is accessible to only a select patient population and carries surgical risk and postoperative nutrient deficiency. Moreover, both pharmacological and surgical treatment strategies don't mechanistically treat IR at the primary cellular signaling event. Exercise remains the gold standard to directly sensitize insulin receptors but suffers from adherence issues and diminished benefit in aging or inflamed physiology[11,12].

Exercise improves insulin sensitivity not only through cellular signaling but also via secreted factors secreted from contracting SkM, including small extracellular vesicles (sEVs). sEVs carry bioactive molecules, including the tetraspanin CD81, a known modulatory protein of intracellular cell signaling which has recently been identified as an influencer of adipocyte morphology and metabolic homeostasis[13]. CD81-enriched sEVs have been detected in WAT following physical activity[14,15], suggesting a novel form of muscle-to-fat communication that could modulate insulin sensitivity.

Despite this emerging evidence, no current therapy specifically leverages or mimics SkM-to-adipose EV signaling. Nor do existing drugs directly address the root defect in IR—disrupted insulin signaling at the membrane. Tetraspanins like CD81 may serve as organizational scaffolds that lower the activation threshold for key signaling pathways, offering new entry points for targeted intervention[16].

SPECIFIC AIMS AND HYPOTHESES

Specific aim #1: To determine if CD81 protein physically interacts with Akt in 3T3L1 preadipocytes.

Hypothesis #1: Protein quantification of immunoprecipitated CD81 from 3T3L1 preadipocytes will reveal co-expression of total Akt1 and pAkt.

Specific aim #2: To determine if silencing CD81 in 3T3L1 preadipocytes impairs insulin signaling.

Hypothesis #2: Compared to scramble siRNA treated 3T3L1 preadipocytes, CD81-siRNA treated 3T3L1 preadipocytes will have decreased expression of phosphorylated Akt.

Specific aim #3: To determine if SkM-derived $CD81^+$ sEVs can restore CD81 content in CD81-silenced 3T3L1 preadipocytes.

Hypothesis #3: Compared to CD81-siRNA treated 3T3L1 preadipocytes treated with a control vehicle, SkM-derived $CD81^+$ sEV treated CD81-silenced 3T3L1 preadipocytes

will have increased expression of CD81, but not to the same magnitude as scramble siRNA treated 3T3L1 preadipocytes.

Specific aim #4: To determine if SkM-derived $CD81^+$ sEVs can improve 3T3L1 preadipocyte insulin signaling.

Hypothesis #4: Compared to 3T3L1 preadipocytes treated with a control vehicle, SkM-derived $CD81^+$ sEV treated 3T3L1 preadipocytes will have increased expression of phosphorylated Akt. Furthermore, compared to CD81-siRNA and SkM-derived $CD81^+$ sEV treated 3T3L1 preadipocytes, scramble siRNA and SkM-derived $CD81^+$ sEV treated 3T3L1 preadipocytes will have the highest expression of phosphorylated Akt.

CHAPTER 2 – CIRCULATING TETRASPANINS: FROM MARKERS TO MECHANISMS DRIVING SYSTEMIC EXERCISE ADAPTATION[1]

The following perspective article, authored by the present master's candidate, was published prior to the completion of the experimental work. It outlines the conceptual framework that inspired the project and highlights the emerging interest in SkM-derived sEVs and CD81 as regulators of adipose tissue insulin sensitivity.

Exercise improves cardiometabolic health through a range of systemic [i.e. beyond working skeletal muscle (SkM)] mechanisms typically attributed to small molecules and peptide hormones. Recent discoveries have shown that the abundance and cargo of circulating small extracellular vesicles (sEVs) like exosomes are altered by exercise, but linking these changes to SkM-derived systemic exercise adaptations has been challenging. A key barrier to linking SkM sEVs to exercise adaptations is determining which of the hundreds of molecules that may be transported by SkM sEVs have functional relevance in the context of exercise. One surprisingly untested strategy is to start with the most abundant sEV cargo. Tetraspanins, like CD81, are transmembrane protein hallmarks of sEVs. To date, CD81 has only been described as an sEV marker, not an instrument of sEV function. However, ~30 yr of research has established CD81 as a transmembrane adaptor protein that influences a variety of cellular functions by altering the organization of receptor proteins within membranes. Multiple groups have recently shown that exercise increases the abundance of circulating sEVs containing

[1] Easterday DS, Lark DS. Circulating Tetraspanins: From Markers to Mechanisms Driving Systemic Exercise Adaptation. Function (Oxf). 2023 Sep 1;4(6):zqad048. doi: 10.1093/function/zqad048. PMID: 37753183; PMCID: PMC10519272.

CD81[14,15] (CD81$^+$ sEVs), which suggests that exercise may increase the delivery of CD81 to recipient cells. Another recent discovery has shown that CD81 supports the preservation of adipose tissue metabolic health during obesity,[13] but it is not known to what extent CD81$^+$ sEVs contribute to this phenomenon. Moreover, no studies to date have described the impact of obesity on the abundance of circulating CD81$^+$ sEVs or what effects circulating CD81 protein may have on recipient cells. In this Opinion, we combine contemporary evidence on exercise-induced circulating sEVs and the metabolic effects of CD81 in adipocytes with historical evidence on cellular CD81 function to propose SkM-to-adipose tissue trafficking of CD81 in sEVs as a novel mechanism driving exercise adaptations.

WHAT EVIDENCE LINKS CD81+ sEVs TO THE PHYSIOLOGY OF EXERCISE?

The study of sEVs and their cargo during exercise is a popular but convoluted area of investigation. Inconsistent isolation methods, various exercise modalities, and different model systems have hindered progress and precluded consensus in the field. This convolution is worsened by a lack of tools to study cell- type-specific (i.e. SkM) sEV populations in vivo. Despite these challenges, some of the strongest evidence linking sEVs to exercise is through CD81. Both progressive[15] and high-intensity interval training[14] exercises acutely increase the circulating abundance of CD81$^+$ sEVs of human subjects (Figure 2A). Brahmer et al.[15] measured CD81 protein from isolated plasma sEVs from young, healthy, and active men at three time points of an incremental cycling exercise protocol: baseline (immediately prior to exercise), during exercise once respiratory quotient (RQ) exceeded 0.9 (which the authors equated to a “moderate”

exercise intensity), and immediately after (< 2 min) cessation of exercise at maximal workload. The authors found that both moderate (RQ ~ 0.9) and maximal intensity exercises increase CD81 protein abundance in circulating plasma sEVs. A more recent study from McIlvenna et al.[14] quantified individual circulating plasma $CD81^+$ sEVs during exercise. In this study young, active, healthy males and females performed high intensity interval training (HIIT) exercise (4 × 30 seconds of cycling at 200% of each participant's predetermined maximal power output). Plasma was collected immediately prior to exercise and < 30 seconds after the final exercise interval. $CD81^+$ sEVs were captured on a microfluidics chip using a CD81-specific antibody and directly quantified using fluorescence detection. Using this more rigorous and direct approach to quantify protein-specific sEV populations, the authors found that HIIT increases the number of circulating $CD81^+$ sEVs. To build upon these promising findings, future studies could explore how long $CD81^+$ sEVs are present in the circulation after exercise, identify the cells (i.e. SkM myofibers) that secrete $CD81^+$ sEVs during exercise, and discover what function(s) they have on recipient cells. It is intuitive and convenient to attribute the effects of exercise on circulating sEVs to SkM myofibers, but there is limited direct evidence to support (or refute) this idea. This knowledge gap exists because there is no known sEV cargo that is exclusive to SkM myofibers, and therefore establishing the mere existence of SkM sEVs in the circulation has been challenging. To address this knowledge gap, our group used a fundamentally different strategy. Instead of trying to find an endogenous SkM- specific sEV cargo, we used Cre-dependent expression of a fluorescent reporter protein in mice to track SkM myofiber-derived sEVs.[17] With this approach, we found that SkM secretes $CD81^+$ sEVs, which reach the circulation. It is not

yet known if, and to what extent, exercise increases circulating SkM CD81$^+$ sEVs or where they might accumulate. However, recent work by Ismaeel et al. found that sEVs containing the muscle (SkM and cardiac)-specific miRNA, miR-1, accumulate in white adipose tissue.[18] These data show that exercise increases circulating CD81$^+$ sEVs, some of which may originate from SkM myofibers, and suggest that white adipose tissue may be a target organ of SkM sEVs secreted during exercise.

HOW MIGHT SKM EVs REACH ADIPOSE TISSUE?

It is not yet clear how sEVs travel from tissues to the blood, but the known anatomical features of the body offer important clues. That is, sEVs are much larger (50-200 nm diameter) than tight junctions of the SkM capillary endothelium (2-3 nm diameter), which should not allow for the passive transendothelial flux of sEVs from the SkM interstitium directly into the circulation (Figure 2B). Moreover, Starling forces dictate that an intact cardiovascular system forces fluid from the capillary endothelium into the interstitial space and subsequently into the lymphatic circulation. Therefore, we believe it is most likely that SkM sEVs reach the blood through the lymphatic circulation. There is experimental evidence for both lymphatic and transendothelial flux of exogenous sEVs, but no studies to date have examined SkM sEV trafficking or established a mechanism of endogenous sEV trafficking from tissues to the blood. Establishing how sEVs from SkM myofibers (and other tissue resident cell types) reach the blood may improve the design and development of tissue-derived sEVs as disease biomarkers and therapeutics. The mechanisms regulating sEV uptake into cells are also incompletely defined. Previous work has shown that adipocytes uptake endothelial cell-derived sEVs

in vitro and in vivo and this process is impaired by overnutrition.[19] In vitro studies have shown that CD81 protein delivered to cultured cells via sEVs is functional,[20,21] which suggests that inter cellular transfer of CD81$^+$ sEVs in vivo allows recipient cells to "adopt" functions attributable to CD81. Future studies are needed to firmly establish the physiological function(s) of CD81$^+$ sEVs on metabolic health and disease outcomes.

WHAT ARE THE CELLULAR FUNCTIONS OF CD81?

CD81 is a transmembrane protein that indirectly enhances adhesion receptor-mediated cellular processes via molecular "webs" [or tetraspanin-enriched microdomains (TEMs)] that aggregate receptors at the cell surface[22] (Figure 1C). The most thoroughly described mechanism of CD81 action is its ability to lower the threshold to activation of B cells and T cells through physical interactions with CD19/CD21 and CD4/CD8, respectively. CD81 is also known to interact with integrin receptors that not only regulate cellular behavior but are also involved in metabolic disease etiology. Recent discoveries by Oguri et al. have demonstrated that CD81 preserves cardiometabolic health via integrin-dependent signaling in white adipose tissue[13]. In their study, the authors demonstrated that CD81 is both necessary and sufficient for de novo beige adipogenesis[13], an adaptation that increases energy expenditure and may be a treatment for obesity and other metabolic diseases. In this same study, the authors discovered that whole-body deletion of CD81 in mice worsened the consequences of diet-induced obesity in white adipose tissue (i.e. fibrosis, inflammation, and insulin resistance) by disrupting integrin signaling. Finally, the authors demonstrated that a low abundance of CD81$^+$ adipocyte progenitor cells within resident white adipose tissue

depots is associated with impaired glucose homeostasis, adiposity, and hypertension in human subjects. The authors did not examine a role for $CD81^+$ sEVs in this study, and it is not yet known how metabolic disease influences the circulating abundance and trafficking of $CD81^+$ sEVs. However, the acute exercise-induced increase in circulating $CD81^+$ sEVs may cause greater delivery of CD81 protein to adipose tissue (and other tissues), thereby contributing to exercise adaptations. Future studies could seek to define the ability of $CD81^+$ sEVs to positively modulate cell signaling pathways necessary for cardiometabolic health. As the body of literature on sEVs continues to grow, it is important to recognize that the systemic effects of sEVs and their cargo are the product of trafficking, abundance, and intracellular function(s). Because CD81 is such an abundant sEV protein, it is possible that its systemic physiological impact when trafficked in sEVs could meet, or exceed, the effects of miRNAs and other scarce sEV cargo that have more tractable molecular mechanisms.

The ability of CD81 to enhance the sensitivity of cell signaling pathways makes it a particularly interesting target for cardiometabolic diseases that are characterized by resistance to second messenger signaling. Based on the evidence provided here, we hypothesize that sEVs contribute to systemic adaptations to exercise via SkM-to-adipose trafficking of CD81. This hypothesis could be tested using emerging transgenic "EV reporter" mouse models[23] and careful study and manipulation of sEV populations in vivo. If $CD81^+$ sEVs are indeed therapeutic, industrial-scale manufacturing of sEVs is already being utilized for numerous clinical trials, so CD81-enriched sEVs could be developed from "bench to bedside" rapidly to improve human metabolic health.

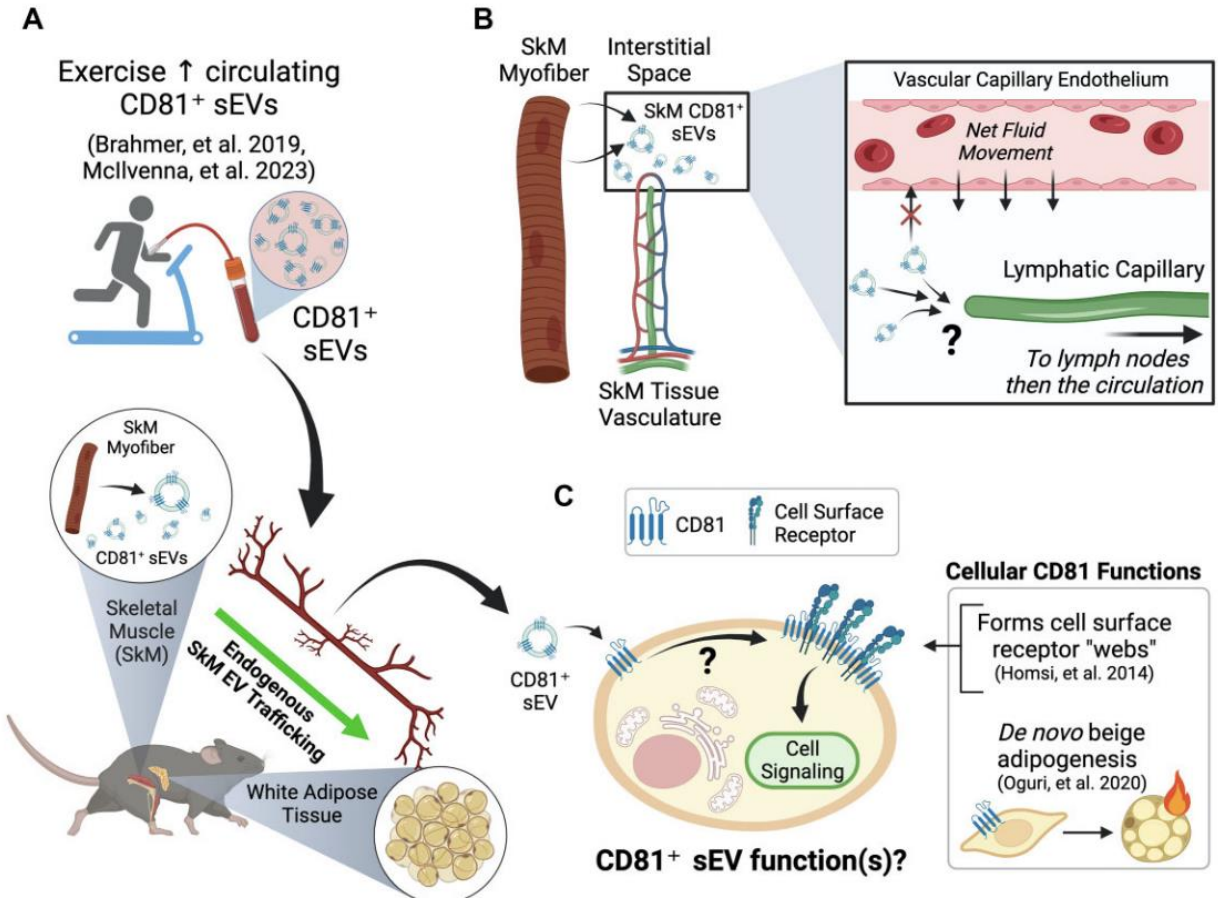

Figure 2. Evidence linking the cellular functions of CD81 to sEVs during exercise. (A) A single bout of continuous aerobic or high-intensity interval training increases CD81+ sEVs in the circulation in human subjects. In mice, SkM myofibers are a major source of CD81+ sEVs reaching the circulation. Endogenous SkM sEVs accumulate in adipose tissue. (B) sEVs are too large to cross endothelial tight junctions, and Starling forces across the capillary endothelium push plasma into the interstitial space. SkM EVs may be taken up by lymphatic capillaries that collect interstitial fluid (which contains sEVs) and transported back to the blood. (C) In cells, CD81 modulates signaling pathways by forming “webs” consisting of CD81 and a variety of cell surface receptors, including integrins (shown). CD81 is necessary and sufficient for de novo beige adipogenesis, which has health-promoting effects on energy expenditure. Future studies could examine whether CD81+ sEVs are capable of regulating signaling pathways and physiological functions already attributed to cell-intrinsic CD81.

CHAPTER 3 – REVIEW OF THE LITERATURE

OBESITY PREVALENCE AND THREAT TO PUBLIC HEALTH

Since the 1960s, the prevalence of obesity in the United States has increased dramatically, tripling from 13% to 40.3% of U.S. adults over the age of 20, with projections indicating that over 50% of the population will be classified as obese by 2030[24]. This rise in obesity correlates with a surge in related chronic health conditions, including type 2 diabetes mellitus (T2DM), cardiovascular disease (CVD), various types of cancer, and neurodegenerative diseases. These obesity-related chronic illnesses, create immense economic burden and is a growing concern to public health. In 2019, the Centers for Disease Control and Prevention (CDC) estimated that obesity-related diseases cost the U.S. healthcare system nearly $173 billion annually[25]. This includes direct medical costs for managing obesity-related conditions like T2DM, CVD, and certain cancers, as well as indirect costs like lost productivity due to illness and disability. Additionally, the obesity epidemic disproportionately affects individuals of low socioeconomic status and racial minorities, exacerbating discriminatory health disparities linked to obesity[24]. The rising obesity rate has placed increasing pressure on both the healthcare system and the economy at large, underscoring the urgent need for comprehensive public health interventions aimed at reversing these trends[26].

Obesity is typically defined by a body mass index (BMI) greater than 30 kg/m^2, a measure that provides a convenient analysis of an individual's total body mass, but does not account for the distribution of adipose tissue as visceral and peripheral fat. A more nuanced definition considers an excessive accumulation of adipose tissue in

relation to lean mass, often quantified by a body fat percentage greater than 35% in adult females and greater than 25% in adult males[27].

The health risks associated with obesity are well-established, with a significantly higher likelihood of individuals with obesity developing IR, which likely precedes and or initiates the onset of obesity-related chronic conditions like T2DM and CVD.

HOMEOSTATIC INSULIN ACTION IN METABOLIC TISSUE

Insulin is a key anabolic hormone regulating glucose homeostasis, lipid metabolism, and protein synthesis. Under physiological conditions, a postprandial rise in blood glucose concentrations stimulates pancreatic beta cells to secrete insulin into the circulation. At the cellular level, insulin binds to the membrane insulin receptor, triggering autophosphorylation of the tyrosine kinase receptor upon ligand interaction. This signals for recruitment and phosphorylation of insulin receptor substrates, which activate phosphoinositide 3-kinase (PI3K). PI3K generates phosphatidylinositol-3,4,5-triphosphate (PIP3), which acts as a binding site for cytosolic Akt (also known as protein kinase B) to the membrane, where it is phosphorylated by phosphoinositide-dependent kinase-1 (PDK1) and the mTORC2 complex. This event triggers activated Akt (pAkt) to dissociate from the membrane and exert key metabolic effects depending on cell of origin, like hepatocytes, myocytes, and adipocytes[4,28]. Due to the positive correlation of insulin receptor activation with the phosphorylation of Akt, pAkt is a logical and convenient marker of insulin sensitivity.

In hepatocytes, insulin action plays a critical role in regulating glucose output to the circulation. Insulin-activated pAkt is translocated to the nucleus, where it phosphorylates FoxO1, a transcription factor required for the transcription of gluconeogenic genes like PEPCK and G6Pase. Phosphorylated FoxO1 is rendered conformationally inactive and exported away from the nucleus, preventing hepatic gluconeogenesis. Hepatic pAkt also phosphorylates cytoplasmic glycogen synthase kinase-3β (GSK3β), rendering it inactive. This eliminates the inhibition of glycogen synthase, allowing for insulin-stimulated glycogenesis. Insulin also promotes hepatic de novo lipogenesis through SREBP-1c activation, which increases transcription of key enzymes such as acetyl-CoA carboxylase (ACC) and fatty acid synthase (FAS), enhancing fatty acid synthesis from glucose-derived intermediates. Simultaneously, insulin suppresses hepatic lipolysis by inhibiting the activity of key lipolytic enzymes, limiting FFA release into circulation[28].

In myocytes, insulin action exerts the same effects as in hepatocytes (i.e., suppresses gluconeogenesis and promotes glycogenesis), with the addition of promoting glucose uptake and protein synthesis. Myocyte pAkt phosphorylates and inhibits cytosolic AS160, a Rab GTPase-activating protein that regulates Rab protein activity of intracellular vesicles. Inhibition of AS160 allows Rab proteins (e.g., Rab8, Rab10, and Rab14) associated with GLUT4-expressing vesicles to become active, enabling vesicle translocation to the plasma membrane and facilitating glucose uptake[29]. Once inside the cell, glucose is used for glycolysis and glycogen synthesis, contributing to reduced blood glucose concentrations. Insulin also activates the mTORC1 pathway through pAkt-mediated inhibition of TSC2, promoting protein

synthesis via phosphorylation of S6K1 and 4E-BP1 and increasing translation of mRNA, essential for SkM maintenance and growth[28].

Insulin action in adipocytes promotes glucose uptake, lipid storage, and suppression of lipolysis. The postprandial nutrient milieu contains high glucose, insulin, and chylomicron-derived triglycerides. Insulin-activated pAkt mobilizes lipoprotein lipase (LPL) to the endothelial surface of the adipose capillary bed, hydrolyzing triglycerides into FFAs and glycerol[30]. FFAs are taken up by surrounding adipocytes and re-esterified using glucose-derived glycerol-3-phosphate (G3P), forming triglycerides for lipid droplet storage. Insulin also stimulates GLUT4 translocation, enhancing glucose uptake. Intracellular glucose supports lipogenesis and triglyceride synthesis more than glycolysis in this tissue. pAkt also promotes adipogenesis through mTORC1 and PPARγ activation, which upregulates genes like adiponectin, FABP4, and LPL while repressing inflammatory pathways like NF-κB[31]. Healthy adipose tissue expansion, or adipogenesis, via hyperplasia (increased number of adipocytes) is associated with improved insulin sensitivity compared to hypertrophic expansion (increased adipocyte size)[32]. Insulin also suppresses lipolysis in adipocytes by inhibiting PKA signaling and dephosphorylating HSL and perilipin-1, preventing lipid mobilization and promoting storage[5,28].

MECHANISMS OF INSULIN RESISTANCE

IR is a pathological condition defined by impaired cellular responsiveness to insulin, resulting in diminished glucose uptake, disrupted lipid metabolism, and altered endocrine signaling. Mechanistically, IR develops from chronic nutrient excess, physical

inactivity, inflammatory stress, and accumulation of intracellular lipid intermediates. A long-standing body of evidence highlights intracellular factors such as serine phosphorylation of insulin receptor substrates, mitochondrial dysfunction, and lipid metabolite accumulation as primary molecular drivers of disrupted insulin signaling[7,33–35]. Specifically, diacylglycerols (DAGs) and ceramides accumulate in insulin-sensitive tissues under high-fat conditions as a result of incomplete fatty acid beta oxidation due to oversaturation of involved enzymes, like carnitine palmitoyltransferase (CPT1), by excess exposure to FFAs. This results in accumulation of lipid intermediates like long-chain acyl-CoAs, which are diverted toward DAG synthesis[35]. Elevated DAGs activate inflammatory protein kinases, like protein kinase C θ (PKCθ), which translocate to the membrane and phosphorylate insulin receptor substrate 1 (IRS-1) on serine residues, thereby preventing insulin signaling due to inhibition of IRS-1 to initiate Akt phosphorylation[33]. Additionally, mitochondrial overload and oxidative stress impair ATP production and increase reactive oxygen species (ROS) production, further disrupting insulin signaling and promoting cellular damage. This can lead to systemic low-grade inflammation that induces expression of pro-inflammatory cytokines (e.g. TNF-α, IL-6) that exacerbate IR through similar stress kinase pathways[34]. Collectively, these maladaptive processes create a feed-forward loop of IR and metabolic inflexibility.

In the liver, IR disrupts hepatic glucose and lipid homeostasis. Under normal conditions, insulin suppresses gluconeogenesis via Akt-mediated inhibition of the transcription factor FoxO1. In insulin-resistant hepatocytes, FoxO1 remains active, sustaining expression of gluconeogenic enzymes like PEPCK and G6Pase, which increases hepatic glucose output. Simultaneously, elevated insulin levels paradoxically

stimulate de novo lipogenesis via the SREBP-1c pathway. This results in unhealthy hepatic lipid accumulation[36], contributing to metabolic-associated steatotic liver disease (MASLD) and hepatocyte IR. Additionally, hepatocyte exposure to inflammatory cytokines and FFA influx from visceral adipose depots activates nuclear factor kappa-light-chain-enhancer of activated B cells (NF-κB) signaling[37], further promoting IR and hepatic dysfunction.

In SkM, the largest site of postprandial glucose disposal, IR results in a failure of GLUT4 translocation to the plasma membrane. Impaired PI3K-Akt signaling leads to sustained activation of AS160, preventing Rab-mediated GLUT4-expressing vesicle mobility[7]. Consequently, glucose uptake into myocytes is significantly reduced, limiting the bioavailable glucose pool for SkM glycogen synthesis and reducing systemic glucose clearance significantly. Chronic lipid exposure, particularly from elevated circulating FFAs, exacerbates this defect. Intramyofibril lipid accumulation and incomplete mitochondrial fatty acid beta oxidation lead to the generation of inflammatory lipid intermediates, including DAGs and ceramides, which interfere with insulin signaling by activating stress kinases such as PKCθ. These kinases promote phosphorylation of IRS proteins, inhibiting their ability to propagate insulin signals via PI3K-Akt signaling[35,38].

Adipose tissue IR significantly contributes to systemic metabolic dysfunction through impaired lipid handling and altered endocrine function. In healthy adipocytes, insulin suppresses lipolysis by inhibiting hormone-sensitive lipase (HSL) and promoting lipid storage through GLUT4-mediated glucose uptake and FFA re-esterification.

However, in insulin-resistant adipocytes, suppression of lipolysis is blunted, resulting in the unchecked release of FFAs into circulation. Elevated circulating FFAs contribute to ectopic lipid deposition in muscle and liver and exacerbate IR systemically. Adipose tissue inflammation, characterized by increased infiltration of macrophages and other immune cells, further disrupts insulin signaling via pro-inflammatory cytokines (e.g. TNF-α, IL-6), which promote serine phosphorylation of IRS-1, preventing the propagation of PI3K-Akt signaling downstream of the insulin receptor[7,39]. Chronic inflammation also promotes extracellular matrix remodeling and fibrotic deposition within adipose depots, which physically impairs insulin diffusion and disrupts endocrine signaling across the tissue. Fibrotic stiffening of the adipose extracellular environment may further impair adipocyte expandability and nutrient/extracellular signal sensing, reinforcing local IR and blunted endocrine responsiveness[40]. Additionally, insulin-resistant adipocytes are shown to have reduced expression and secretion of adiponectin, a key insulin-sensitizing molecule that enhances fatty acid oxidation and improves systemic insulin sensitivity[31]. Simultaneously, circulating leptin levels rise with increasing adiposity, yet central leptin signaling becomes less responsive, creating an environment of "leptin resistance" that impairs appetite regulation and decreases energy expenditure[41].

It is notable that the collapse of lipid handling in obese adipose tissue allows for an expansive and uncontrolled release of FFAs into the circulation that has extreme deleterious effects on other metabolically active tissues, like SkM and liver, as well as promoting obesogenic adipose tissue migration into the viscera. This lipotoxic cascade debatably propagates the greatest burden to the insulin resistant cycle[8], that of

incomplete lipid handling in many tissues, therefore pointing to adipocytes as a logical target for investigating novel treatments for whole-body IR.

CLINICAL INSULIN RESISTANCE AND CURRENT THERAPEUTIC STRATEGIES

Systemically, IR precedes and contributes to a constellation of cardiometabolic diseases. Hyperglycemia and hyperinsulinemia drive endothelial dysfunction, increase vascular stiffness, and elevate blood pressure. Chronic elevation of FFAs contributes to atherogenic dyslipidemia, characterized by increased triglycerides, decreased HDL, and increased small dense LDL particles. These alterations accelerate the development of atherosclerosis, cardiovascular disease, and exacerbate risk for stroke and myocardial infarction[42]. Moreover, chronic low-grade inflammation associated with IR is implicated in the progression of neurodegenerative diseases and certain cancers[43]. Thus, IR represents not only a tissue-specific metabolic impairment but also a systemic pathological state that underpins multiple chronic diseases. Current therapeutic strategies for IR include pharmacologic agents, bariatric surgery, and exercise with caloric manipulation. GLP-1 receptor agonists (e.g., semaglutide, liraglutide) improve glycemic control and induce weight loss, but can plateau in efficacy over time and are associated with gastrointestinal side effects[9]. SGLT2 inhibitors (e.g., empagliflozin, dapagliflozin) promote glucose excretion and improve cardiovascular outcomes but do not directly target insulin signaling at the cellular/tissue level[10]. Bariatric surgery induces significant metabolic improvement, weight loss, and improved insulin sensitivity, but is invasive, financially inaccessible, and associated with long-term nutritional deficiencies that greatly effect quality of life[44]. Exercise remains the most comprehensive non-

pharmacologic therapy, directly enhancing insulin receptor sensitivity and promoting systemic metabolic health[45], but it requires high adherence and may be less effective in individuals with advanced disease or physical limitations. Collectively, these limitations highlight the need for more targeted, tissue-specific therapies that directly improve insulin receptor function upstream of Akt phosphorylation.

CD81 AS A MEDIATOR OF CELL SIGNALING

To investigate potential mediators of insulin receptor signaling, it is logical to start with other membrane associated molecules, and more specifically, a family of proteins that is widely expressed in all cell types yet largely understudied in the context of cell metabolism: tetraspanins. Broadly, tetraspanins (like CD81, CD9, CD82, CD151) self-associate with integrins, growth factor receptors, lipids, and other tetraspanins by physically reorganizing within the plasma membrane in what is termed a tetraspanin-enriched microdomain (TEMs)[46]. Membrane-associated TEMs function to bring together receptors and kinases to propagate rapid signal transduction across the membrane and to facilitate cell adhesion/motility. Tetraspanins contains two extracellular loop domains (EC1 and EC2) and two cytosolic termini[47,48], which structurally allows the proteins to dually interact with membrane partner proteins and with intracellular factors. CD81 is widely ubiquitous tetraspanin relative to others, as it is expressed in nearly all cell types and is found abundantly circulating on exosomes[49]. While the mechanistic functions of CD81 are largely unknown, a few studies have demonstrated functional roles of CD81 in various tissues. Upon its discovery by the late Dr. Shoshana Levy in 1990[50], CD81 was first identified by an immunoprecipitation assay intended to define cell surface

molecules involved in cell growth regulation, specifically in human B-cells[51]. Levy et al. found that CD81 is a critical component of lowering B-cell activation thresholds via direct interactions with partner protein CD19[52]. CD81 is also demonstrated to physically interact with various integrins[53] to regulate T-cell adhesion, migration, and antigen presentation[54]. Complete or partial loss of CD81 has a wide array of immune and endocrine fluctuations. A human genetic mutation for homozygous CD81 resulting in CD81-null blood leukocytes revealed B-cells with impaired activation upon antigen exposure[55], while complete knockout of CD81 (CD81-KO) in mice yields sterile females and disrupted Mendelian distribution of CD81 alleles in the offspring of CD81-KO males[56]. Contrarily, CD81 is required for viral DNA replication and the formation of viral particles in herpes simplex virus 1 (HSV1) and CD81-KO cell lines reveal impaired HSV1 infection[57].

EMERGING ROLES OF CD81 IN METABOLISM

The function of CD81 as a mediator of antigen recognition and systemic immune response is clear, yet the roles of this ubiquitous protein beyond immune cell function has not been well researched until recently. In 2020, Oguri et al.[13] published findings that establish CD81 as essential to maintaining healthy adipose tissue proliferation. Using RNA sequencing, investigators identified that $CD81^{+}$ adipocyte progenitor cells (APCs) derived from C57BL6 mice were more proliferative and more likely to differentiate into “beige” adipocytes than CD81- APCs. The authors further discovered that CRISPRi-CD81 mice had significantly less proliferative/beige APCs in the WAT than littermate controls, suggesting CD81 is required be *de novo* beige adipogenesis.

“Beiging” of WAT is an adaptive cellular process in which an increase of mitochondria-enriched adipocytes with multi-locular lipid droplets emerge in the WAT in response to sympathetic stimulation, like a cold exposure. These beige adipocytes express high uncoupling protein 1 (UCP1), which acts to uncouple the mitochondrial membrane to allow protons to leak as heat rather than used to generate ATP[58]. This non-shivering thermogenic adaptation acutely increases the WAT energy expenditure and thus is an attractive outcome to combat obesity and IR. Interestingly, the authors also found that aged mice (60 weeks old) had significantly fewer $CD81^+$ APCs than young mice (8-10 weeks), implying that age decreases the proliferative and beiging capacity of APCs.

Arguably the most compelling, the authors[13] also found that whole body loss of CD81 using CRISPR/CAS9 caused mice to gain significantly more body weight on just 3 weeks of a high-fat diet (HFD) as compared to littermate controls, despite no difference in activity between genotypes. CRISPRi-CD81 mice became glucose intolerant at 8 weeks of HFD as compared to littermate controls, and these mice expressed significantly higher inflammatory and pro-fibrotic genes as compared to littermate controls. To round out this lucrative study, the authors obtained human subcutaneous WAT across a wide BMI range and found that the percentage of $CD81^+$ APCs inversely correlates with HOMA-IR, fasting blood glucose levels, and diastolic blood pressure[13]. All of these findings together elucidate a clear and clinically significant role of CD81 in regulating adipocyte energy expenditure, morphology, and proliferation with greater systemic outcomes.

The role of CD81 as a biomarker of extracellular vesicles (EVs) is well-established in the literature[49], so much so that many EV isolation techniques either capture CD81 directly or measure its presence as a validation metric of EV enrichment. However, the functional role of CD81 when delivered to a target cell in an EV remains undefined.

EXTRACELLULAR VESICLES: DEFINITIONS AND CHALLENGES

EVs are lipid bilayer-bound vesicles secreted by virtually all cell types, and they are broadly classified by size and biogenesis: Exosomes, a subtype of small EVs (sEVs), are typically <200 nm and originate from endosomal multivesicular bodies, often carrying proteins such as tetraspanins (CD81, CD63, CD9), heat shock proteins, and ESCRT-related machinery, along with lipids, mRNA, and miRNAs. Microvesicles, a subtype of large EVs (lEVs), are generally >200 nm and formed by outward budding of the plasma membrane, reflecting the cytoplasmic environment of the origin cell. Apoptotic bodies, also large EVs, are usually >1000 nm and are released from dying cells, containing organelle fragments and nuclear debris[59].

EVs can be isolated through multiple techniques, each with inherent trade-offs in yield, purity, and functional preservation. Ultracentrifugation is the most commonly used method but may co-pellet protein aggregates or damage EV membranes due to high centrifugal forces. Size exclusion chromatography (SEC) offers superior purity by separating EVs based on size and preserving functional integrity, but total EV yields can be lower. Immunoaffinity capture, such as magnetic bead-based isolation using CD81 antibodies, provides high specificity for a subpopulation of EVs but at the expense of

decreased yield and the potential of altered EV functionality through competing binding interactions with the capture antibody.

Despite advances in isolation, challenges in EV research remain. The heterogeneity of EV populations makes it difficult to attribute observed functional outcomes to a specific vesicle subtype or cargo molecule. For example, it is common to collect EVs from cell culture due to the convenience of one origin cell type as opposed to collecting EVs from whole tissue or blood *in vitro* or *ex vivo*. However, even the single cell heterogeneity of proteins, lipids, and nucleic acids complicates identifying individual functions of EV-associated cargo. Additionally, isolation methods based upon size exclusion do not necessarily exclude non-EV particles of similar size. There is also a lack of standardization across isolation protocols used in various fields of EV research, making cross-study comparisons difficult. These limitations have led to the Minimal Information for Studies of Extracellular Vesicles (MISEV) guidelines, which recommend using descriptive terms like "small extracellular vesicles (sEVs)" when subcellular origin is not definitively confirmed[59]. In accordance with these guidelines, this thesis will refer to the CD81-enriched EV population as sEVs, based on their size and CD81 content, while avoiding the term "exosome" due to the absence of biogenesis or machinery-based validation. Figure 3 graphically outlines the experimental approach used in the

present study that was chosen to align with the latest recommendations from EV research experts[60].

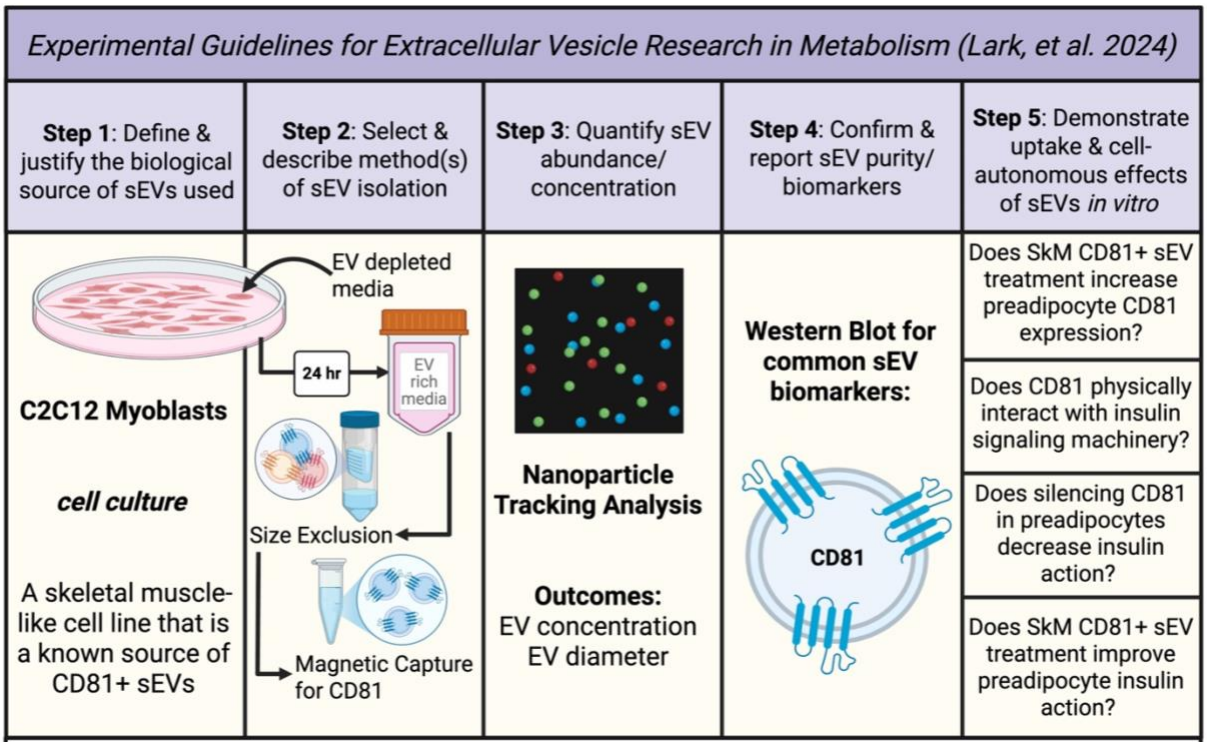

Figure 3: Experimental workflow of capturing, quantifying, and investigating SkM-derived CD81+ sEVs in accordance with field recommendations

SKELETAL MUSCLE AS A SOURCE OF CD81$^+$ EVs TO ADIPOSE TISSUE

Not only is skeletal muscle (SkM) the largest insulin-sensitive tissue in the body by mass, but also a robust endocrine organ capable of secreting a wide array of signaling factors termed myokines[61], including EVs. Our laboratory provided novel evidence that SkM-derived EVs reach the circulation *in vivo,* and that SkM secretes more EVs into the circulation than WAT using a Cre-dependent SkM-reporter mouse[17].

Ismaael et al. demonstrated that sEVs containing muscle-specific miRNA miR-1 preferentially accumulate in WAT. The endocrine action of SkM is largely responsive to exercise, and exercise-induced SkM-secreted factors are metabolo- and cardioprotective in recipient tissue. A growing body of evidence suggests that exercise acutely increases the circulating abundance of $CD81^+$ sEVs of human subjects, and that this adaptation is largely from the SkM. Brahmer et al. measured CD81 protein levels in plasma sEVs from young, healthy, active men at three timepoints: baseline (pre-exercise), during moderate-intensity exercise (when RQ > 0.9), and immediately post-exercise at maximal effort. They found that both moderate and maximal exercise significantly increased CD81 abundance in circulating sEVs[15]. A different study by McIlvenna et al. directly quantified circulating $CD81^+$ sEVs in young, healthy males and females undergoing high-intensity interval training (HIIT; 4 × 30s cycling bouts at 200% max power). Plasma was collected immediately before and within 30 seconds after exercise. Using a microfluidics chip with CD81-specific antibody capture and fluorescence detection, they identified that HIIT significantly increases the number of circulating $CD81^+$ sEVs[14]. Obi et al. provided evidence from cultured myotubes that skeletal muscle secretes EVs during and after exercise (electrically paced contractions), and exercised cells secrete more small EVs expressing higher CD81 than non-exercised cells[62], substantiating prior works by Brahmer et al. and McIlvenna et al. while strengthening the argument that SkM myofibers are at least in part responsible for significant changes in secreted $CD81^+$ sEVs. Collectively, this body of data suggests that exercise increases circulating $CD81^+$ sEVs, some of which were secreted from SkM myofibers, and that SkM-derived $CD81^+$ sEVs may be targeted to WAT during exercise.

Paired with the findings from Oguri et al., wherein the number of CD81$^+$ adipocytes present in subcutaneous WAT is inversely correlated with markers of insulin resistance (HOMA-IR, fasting blood glucose)[13], it is logical to question if SkM-derived CD81$^+$ sEVs are physiologically relevant sources of CD81 to adipose tissue as a metabolically protective myokine.

CD81$^+$ sEVs AS THERAPEUTICS: STRENGTHS AND LIMITATIONS

EVs are readily internalized by recipient cells via several pathways, including receptor-mediated endocytosis, macropinocytosis, and in some cases, direct membrane fusion[63]. While the exact mechanisms governing adipocyte EV uptake remain poorly defined, the known functions of tetraspanins and TEMs as mediators of cell motility and adhesion[53,57] support the potential for EV surface proteins such as CD81 to facilitate EV internalization or initiate signaling cascades upon membrane contact. Clinically, EV-based therapies are under investigation for cancers, neurodegenerative diseases, and cardiovascular conditions. They have emerged as an attractive therapeutic strategy for several reasons: EVs are inherently biocompatible and protected by a lipid bilayer, allowing for the safe delivery of either native or pharmacologically loaded cargo. They can also cross biological barriers, a key advantage over many traditional therapeutics. However, the promise of EV-based therapies comes with unique challenges. Isolation methods remain unstandardized and often low yield, raising concerns about scalability for clinical applications. Moreover, ensuring quality control and safety presents major regulatory hurdles, as EVs are biologically derived and highly heterogeneous. As with

other biologics, batch-to-batch consistency must be tightly monitored, requiring rigorous validation and oversight before therapeutic approval.

The functional implications of protein delivery via EVs is promising, as membrane-bound proteins like CD81 are structurally and functionally conserved in the membrane and integrated into the recipient cell membrane. Given the evidence supporting CD81 as a significant mediator of metabolic activity in WAT[13], we hypothesize that delivery of CD81 via EVs could potentially donate enough functional CD81 to improve adipocyte insulin signaling. Downstream of this hypothesis, If loss of CD81 causes diet-induced obesity and IR in mice, perhaps restoring CD81 via exogenous EV delivery could reverse this. The proximity of CD81 within the membrane to the insulin receptor and it's ability to fine-tune intracellular signaling contributes to the novelty of this approach as compared to other therapeutic strategies. It is important to acknowledge that $CD81^+$ sEVs contain an unknown diversity of molecular cargo that may also have effects on recipient tissue, and investigating this effect is a future direction of this project. $CD81^+$ SkM-derived sEVs may represent a next-generation, tissue-targeted approach to re-sensitize insulin-resistant adipose tissue. By leveraging the physiological communication axis between SkM and WAT, these vesicles could unlock a novel therapeutic pathway for restoring metabolic balance at its primary source.

CHAPTER 4 – PRELIMINARY DATA

This chapter presents preliminary findings from the candidate's prior undergraduate research and unpublished experiments from the Extracellular Regulation of Metabolism Laboratory that informed the current investigation into SkM-derived $CD81^+$ sEVs and adipocyte insulin sensitivity.

PRELIMINARY STUDY 1 - RATIONALE

Preliminary study 1 was inspired by the findings of Oguri et al.[13] and was intended to study phenotypic changes in primary adipocyte progenitor cells (APCs) derived from murine inguinal WAT (iWAT) treated directly with $CD81^+$ sEVs derived from the SkM of the same animal in vitro. Specifically, we aimed to investigate the potential of SkM-derived $CD81^+$ sEVs to influence adipocyte differentiation and induce a beiging phenotype in vitro. Due to beige adipogenesis characterization as proliferative, small adipocytes with multi-locular lipid droplets, lipid droplet abundance and diameter were measured as primary outcomes.

PRELIMINARY STUDY 1 - METHODS

Three Male and two female C57BL/6 mice were used as the source of both iWAT-derived APCs and skeletal muscle tissue. APCs were isolated using a magnetic labeling protocol to deplete non-adipogenic cells and positively select for progenitor cells. SkM-derived $CD81^+$ EVs were isolated ex vivo from muscle tissue of the same mouse using size exclusion chromatography followed by magnetic capture. Once established in culture, APCs were differentiated in vitro in the presence or absence of $CD81^+$ SkM EVs and/or the exogenous beiging agonists norepinephrine and rosiglitazone in order to

replicate the sympathetic activation used in Oguri et al. animal studies[13]. Four treatment groups were used per mouse sample: a vehicle control, CD81⁺ EV treatment alone, beiging agonist treatment alone, and a combined CD81⁺ EV with beiging agonist group. Notably, EVs and APCs were matched by biological donor to preserve tissue-specific signaling context. Over a 16-day time course, adipocyte morphology and lipid droplet maturation were monitored via brightfield microscopy, and lysates were collected at endpoint for downstream protein analysis. These early findings helped shape the rationale and experimental framework for the current thesis work.

PRELIMINARY STUDY 1 – RESULTS

SKM-DERIVED CD81⁺ sEVs TREATMENT INCREASES LIPID DROPLET ABUNDANCE IN ADIPOCYTE PROGENITOR CELLS

APCs treated with SkM-derived CD81⁺ sEVs contained more lipid droplets than APCs that received a control vehicle, both in the presence and absence of beiging agonists treatment ($p=0.0287$) (Preliminary Data Figure 4A). A trend was observed for smaller lipid droplet diameters in APCs treated with SkM-derived CD81⁺ sEVs when compared to non-EV treated controls. Contrastingly, there is a trend towards larger lipid droplet diameters in SkM-derived CD81⁺ sEV treated cells in the presence of beiging agonists, though a lack of statistical significance demands further evidence to draw this conclusion (Preliminary Data Figure 4B).

PRELIMINARY STUDY 1 – DISCUSSION AND RELATION TO CURRENT PROJECT

Preliminary study 1 identified that APCs treated with SkM-derived CD81⁺ sEVs contain significantly more lipid droplets than untreated APCs whether in the presence or

absence of sympathetic agonists (Preliminary Data Figure 4A). This finding suggests that SkM-derived CD81 EVs increase the proliferation of “beige” adipocytes, or de novo beige adipogenesis. However, it is important to recognize that this data presents lipid droplets per well rather than lipid droplets per cell, as no nuclear stain was used to count cells per well. Though this is a limitation to interpreting this data, it remains plausible that SkM-derived CD81+ sEVs increased APC proliferation and/or adipogenesis as the expansion of new adipocytes is a well-established primary function of APCs[64]. This hyperplasic, as opposed to hypertrophic, expansion of adipocytes is consistent with improvements in adipose energy storage homeostasis and should not be interpreted as a deleterious expansion of WAT[32]. These findings further substantiate that SkM-derived $CD81^+$ sEVs exert functional affects in adipocytes reflected by morphological changes consistent with more energetically active adipocytes.

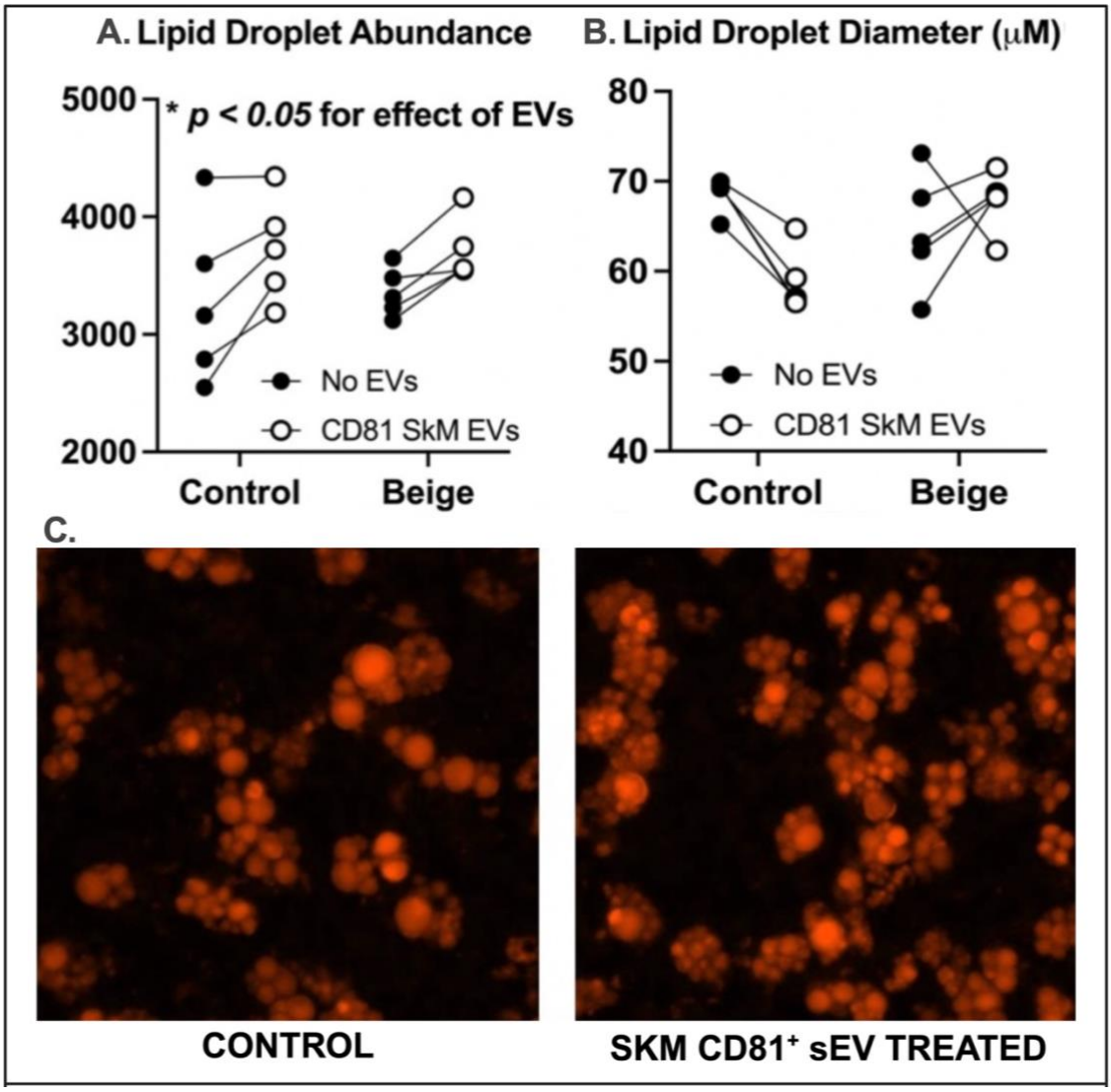

Figure 4: Preliminary Data. (A) Lipid droplet abundance (lipid droplets/well) under control conditions and beiging conditions (norepinephrine and rosiglitazone) with or without SkM-derived CD81⁺ sEV treatment. (B) Lipid droplet diameter (μM) under control conditions and beiging conditions (norepinephrine and rosiglitazone) with or without SkM-derived CD81⁺ sEV treatment. (C) 20x fluorescent phase contrast microscopy representative images of stained lipid droplets after 16 days of differentiation. On the left, APCs grown in non-beiging conditions without SkM-derived CD81⁺ sEV treatment. On the right, APCs grown in non-beiging conditions with SkM-derived CD81⁺ sEV treatment.

PRELIMINARY STUDY 2 – RATIONALE

Preliminary study 2 serves as an extension of our laboratory's work using the "mT/mG" mouse, a transgenic SkM-specific EV reporter mouse previous described by Estrada et al[17] (Preliminary Data Figure 2A), wherein all EVs secreted by SkM myofibers express enhanced green fluorescent protein (eGFP). Following the discovery that SkM-derived sEVs reach the circulation *in vivo,* our laboratory initially aimed to elucidate the accumulation of SkM-derived sEVs in different regional fat pads. Subsequently, we also aimed to define the effect of diet-induced obesity (DIO) on the magnitude of SkM secretion of $CD81^+$ sEVs and the abundance of circulating $CD81^+$ EVs using the same mouse model.

PRELIMINARY STUDY 2 – METHODS

To assess SkM-derived sEV accumulation in different regional fat pads, mT/mG SkM EV reporter mice were sacrificed and three fat pads were collected: perigonadal adipose tissue (pWAT), brown adipose tissue (BAT), and inguinal adipose tissue (iWAT). Tissues were analyzed by ELISA assay to measure eGFP expression in each fat pad.

To assess the effects of DIO on the secretion of $CD81^+$ SEVs from the SkM and the abundance of circulating $CD81^+$ sEVs, we fed mT/mG SkM EV reporter mice a HFD or chow diet for 3 weeks prior to sacrifice and collection of plasma and tissues. To measure local secretion of $CD81^+$ sEVs from SkM, vastus medialis tissue was allowed to secrete EVs into EV-depleted media overnight ex vivo, as described by Estrada et al[17]. Plasma EVs and SkM-derived EVs were quantified for CD81 using Exoview technology, a single-particle tetraspanin antibody-linked detection system.

PRELIMINARY STUDY 2 – RESULTS

SKELETAL MUSCLE DERIVED sEVs PREFERENTIALLY ACCUMULATE IN WHITE ADIPOSE TISSUE

ELISA analysis of various adipose tissue depots revealed significant eGFP expression in all WAT samples, demonstrating that SkM-derived eGFP is transferred to WAT *in vivo* (Figure 5A).

DIET-INDUCED OBESITY INCREASES SKM SECRETION OF CD81⁺ sEVS BUT DECREASES CIRCULATING CD81⁺ sEVS

Exoview analysis of SkM-derived CD81⁺ sEVs revealed that SkM from HFD fed mice secrete more CD81⁺ sEVs than SkM from chow diet fed mice *ex vivo* (Figure 5B), while Exoview analysis of plasma-derived CD81⁺ sEVs revealed that HFD fed mice have less circulating CD81⁺ sEVs than chow fed mice (Figure 5C).

PRELIMINARY STUDY 2 – DISCUSSION AND RELATION TO CURRENT PROJECT

Preliminary study 2 provided data that substantiated findings from others while also identifying novel effects of DIO on SkM sEV secretion and circulating sEVs. Our evidence that SkM-derived sEVs preferentially accumulate in WAT (Figure 5A) aligns with previous work from Vechetti et al. who found that exercise induces the secretion of muscle-specific miR-1 containing EVs that are preferentially taken up by WAT[65]. This preliminary study also identified a novel effect of DIO on SkM secretion of CD81⁺ sEVs, wherein DIO increases the secretion of CD81⁺ sEVs, while also identifying that circulating CD81⁺ sEVs decrease during DIO. Contrastingly, others have demonstrated that exercise increases circulating CD81⁺ sEVs[14,15]. Taken together, these data suggest

that changes in circulating CD81 may predict systemic metabolic health, and SkM may play a compensatory role in providing a systemic pool of CD81⁺ sEVs, some of which is largely targeted to WAT.

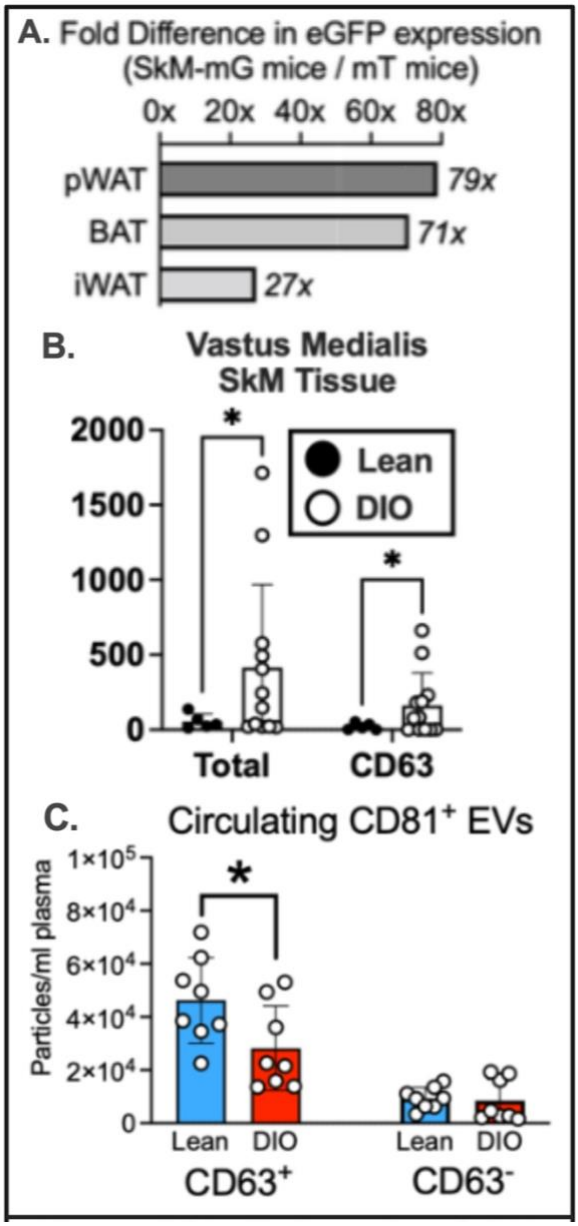

Figure 5: Preliminary data. (A) eGFP expression is perigonadal, brown, and inguinal adipose tissue depots collected from mT/mG SkM EV reporter mice. (B) DIO increases SkM secretion of CD81⁺ sEVs *ex vivo* (n=8 mice/group). (C) DIO decreases circulating CD81⁺ sEVs *in vivo.*

CHAPTER 5 – METHODOLOGY

C2C12 EV Collection

C2C12 myoblasts were cultured to obtain extracellular vesicle (EV)-containing conditioned media (CM). Cells were grown in 80% DMEM, 19% fetal bovine serum (FBS), and 1% penicillin-streptomycin until fully confluent in three T150 flasks. Media was replaced with 30 mL of EV-depleted media per flask (90% DMEM, 9% EV-depleted One Shot, 1% pen/strep), and CM was collected after 24 hours. The media was then replaced for another 24 hours and collected again. This process was repeated, yielding ~360 mL total CM. CM was centrifuged at 500 × g for 5 min, followed by 2000 × g for 5 min, and 4000 × g for 15 min to remove cell debris and larger vesicles.

sEV Isolation by Size Exclusion Chromatography (SEC)

The CM was concentrated using 100 kDa MWCO filters to generate a retentate (>100 kDa) and filtrate (<100 kDa). The retentate was processed through Capto Core 700 columns. The resin, pre-washed with cold DPBS, traps hydrophobic and positively charged contaminants under 700 kDa, allowing sEV-sized particles to elute. The column was washed with DPBS to recover any remaining vesicles. The collected sEV fractions were pooled and concentrated again using 100 kDa filters and stored at -20°C. An aliquot was saved for downstream analysis.

SEC-Isolated sEV Quantification

Aliquots of concentrated sEVs were analyzed by nanoparticle tracking analysis (NTA; Horiba ViewSizer 3000). Samples were diluted in 0.1 µm-filtered water to reach 100–

150 tracks/frame. Specific frame and laser settings were used to calculate sEV concentrations. Because NTA is incompatible with magnetic beads, $CD81^+$ sEVs were instead quantified using a Horiba Aqualog fluorescence spectrometer. Protein-associated fluorescence at 281 nm was used to approximate protein concentration and compared between $CD81^+$ sEVs and their depleted flow-through counterparts.

$CD81^+$ sEV Isolation

$CD81^+$ sEVs were isolated using magnetic-activated cell sorting (MACS). SEC-isolated sEVs were incubated with CD81 antibody-conjugated microbeads for 1 hour at room temperature, then loaded onto MACS columns under a magnetic field. Retained $CD81^+$ sEVs were eluted in 2.5 mL of DMEM. An equivalent mock control was prepared using DPBS. Based on total NTA quantification, $CD81^+$ sEVs were estimated to contain ~5×10^{11} particles.

CD81 Silencing in 3T3L1 Preadipocytes

3T3L1 preadipocytes were grown in 79% DMEM, 20% FBS, and 1% pen/strep. Cells at 70% confluency were transfected with CD81-targeting or scramble siRNA using Lipofectamine in opti-MEM. Final transfection media contained 0.01 nM siRNA and 0.283% Lipofectamine per well. Transfection was carried out for 24 hours.

Immunoprecipitation of CD81 and Akt from 3T3L1 preadipocytes

A separate cohort of 3T3L1 preadipocytes was grown in 79% DMEM, 20% FBS, and 1% pen/strep to 100% confluence. Media was switched to 100% DMEM to induce a 4

hour period of insulin starvation prior to half of these cells receiving 100 nM of bovine insulin for 15 minutes. Cell lysates were collected in ice-cold non-denaturing lysis buffer (PBS + 0.1% Triton X-100 + 1% HALT), combined, then incubated with agitation @ 4C for 30 minutes. Samples were centrifuged @ 10,000 x g for 10 minutes to pellet nuclei and cell debris. 50 ul of CD81 capture antibody (Miltenyl Biotec) was added and mixtures were incubated with agitation @ 4C for 2 hours. Samples were prepped for western blotting and equal volumes were run for gel electrophoresis and immunoblotting for Thr^{308} Akt.

Treatment with $CD81^+$ sEVs

Twenty-four hours after transfection, 50 µL of $CD81^+$ sEVs (~1×10^{10} particles) or control vehicle were added to respective wells. After 24 hours, wells were washed and re-dosed with an additional 50 µL of $CD81^+$ sEVs or control vehicle in insulin-free DMEM (100% DMEM) for 6 hours.

Insulin Dosing

Following a 6 hour insulin starvation in 100% DMEM, cells were treated with 0 M, 100 nM or 1 µM bovine insulin dosed in 50 µL of DMEM for 15 minutes, bringing total well volume to 1 mL and total well concentrations to 0 nM, 10 nM, and 100 nM.

Sample Collection

Media was collected, and cells were washed with ice-cold DPBS. Cell lysates were collected in 110 µL RIPA buffer with 1X HALT protease and phosphatase inhibitor,

incubated on ice for 20 minutes, and centrifuged at 13,000 × g for 20 min at 4°C. Supernatants were stored at -20°C.

Protein Quantification

Protein concentrations were determined by BCA assay. Lysates were diluted 1:10, incubated with BCA reagent at 37°C for 30 minutes, and absorbance was measured at 562 nm. Concentrations were calculated from a BSA standard curve.

Western Blot

Protein lysates were prepared at 1 µg/µL and 30 µg were loaded per lane on 4–12% Bis-Tris gels. Gels were run at 130 V, and proteins were transferred to nitrocellulose membranes. Membranes were stained with Ponceau, blocked in 5% BSA, and incubated overnight at 4°C with the following primary antibodies: CD81, pAkt, total Akt, CD63, and UCP1. After TBST washes, membranes were incubated with HRP-conjugated secondary antibodies and developed using SuperSignal™ West Femto substrate. Bands were imaged and quantified using ImageJ/Fiji. Targets (CD81 and pAkt) were normalized to total Akt expression.

Statistics

All data are presented as mean values of protein band density +/- standard error of the mean (SEM). Unpaired, two-tailed Student’s t-tests were employed to compare differences between two groups (i.e. sEV-treated vs. no sEVs). A p-value of less than 0.05 was considered statistically significant. Statistical analyses and graph generation

were performed using Prism. For comparisons involving more than two groups, one-way ANOVA followed by Tukey's post hoc test (if necessary) was used.

CHAPTER 6 – RESULTS

CD81$^+$ sEV COLLECTION RESULTS

Total C2C12-derived sEVs isolated by size exclusion chromatography (SEC) were quantified with nanoparticle tracking analysis (NTA). The concentration of sEV sized particles isolated by SEC was 8.4E+10 particles/mL in 6 mL of diluent, for a total of 5.04E+11 particles isolated. Average particle size was 94 nm +/- a standard deviation of 43 nm, and modal particle size was 64 nm (Supplementary Figure 1). These values are consistent with sEVs that we and others have previously reported.

NTA cannot be performed on magnetically captured CD81$^+$ sEVs due to the use of magnetism to mix samples in the Horiba Viewsizer.

AIM #1 RESULTS – CD81 PROTEIN PHYSICALLY INTERACTS WITH P-Akt IN 3T3L1 PREADIPOCYTES

To investigate whether CD81 interacts with Akt in preadipocytes, CD81 was immunoprecipitated from non-denatured lysates using the same magnetic beads used to capture CD81+ sEVs (*see Methods*). Western blot analysis revealed abundant expression of pAkt in CD81-captured protein complexes (Figure 6). This demonstrates that CD81 physically associates with pAkt in 3T3L1 preadipocytes.

AIM #2 RESULTS – CD81 SILENCING DOES NOT SIGNIFICANTLY IMPAIR INSULIN ACTION IN 3T3L1 PREADIPOCYTES

To determine whether CD81 is necessary for insulin signaling in adipocytes, 3T3L1 preadipocytes were treated with CD81 siRNA or scramble control and stimulated with insulin. CD81 siRNA robustly decreases expression of CD81 in 3T3L1 preadipocytes (p-value < 0.0001) (Figure 7A). Western blot analysis of pAkt/tAkt revealed no statistically significant difference in insulin action between CD81-silenced and scramble preadipocytes (Figure 7B). However, a modest reduction in pAkt expression was observed in CD81-silenced preadipocytes, suggesting a potential trend toward blunted insulin signaling. These results indicate that while CD81 silencing does not significantly impair insulin action under the tested conditions, further investigation may be warranted.

AIM #3 RESULTS – SKM-DERIVED CD81$^+$ sEVS RESTORE CD81 CONTENT IN CD81-SILENCED PREADIPOCYTES

SkM-derived CD81$^+$ sEVs increased CD81 protein content in CD81-silenced 3T3L1 preadipocytes, but not controls treated with scrambled siRNA (p-value < 0.05) (Figure 8). These results support the hypothesis that CD81$^+$ sEVs can deliver CD81 protein to 3T3L1 preadipocytes.

AIM #4 RESULTS – SKM-DERIVED CD81$^+$ sEVS DO NOT SIGNIFICANTLY IMPROVE INSULIN ACTION IN 3T3L1 PREADIPOCYTES

Treatment with SkM-derived CD81$^+$ sEVs did not significantly increase insulin action (pAkt/tAkt) when compared to vehicle-treated controls (Figure 9). Further investigation into different CD81$^+$ sEV isolation methods, sEV dose, timing, or additional factors influencing sEV efficacy is warranted.

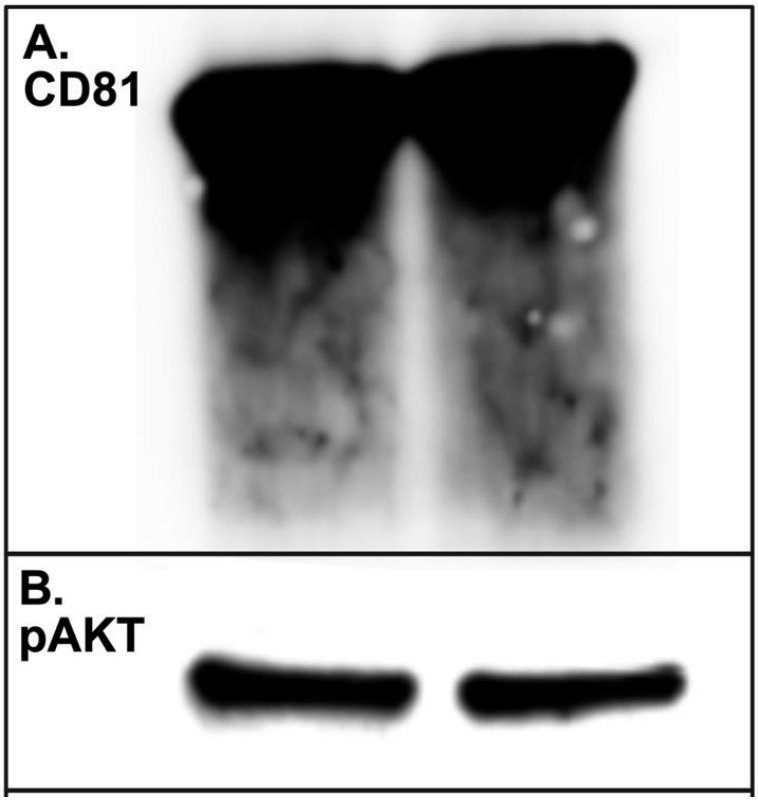

Figure 6: CD81 protein physically interacts with pAKT in 3T3L1 preadipocytes. (A) CD81 expression in 3T3L1 preadipocytes after CD81 immunocapture. (B) pAKT expression in 3T3L1 preadipocytes after CD81 immunocapture.

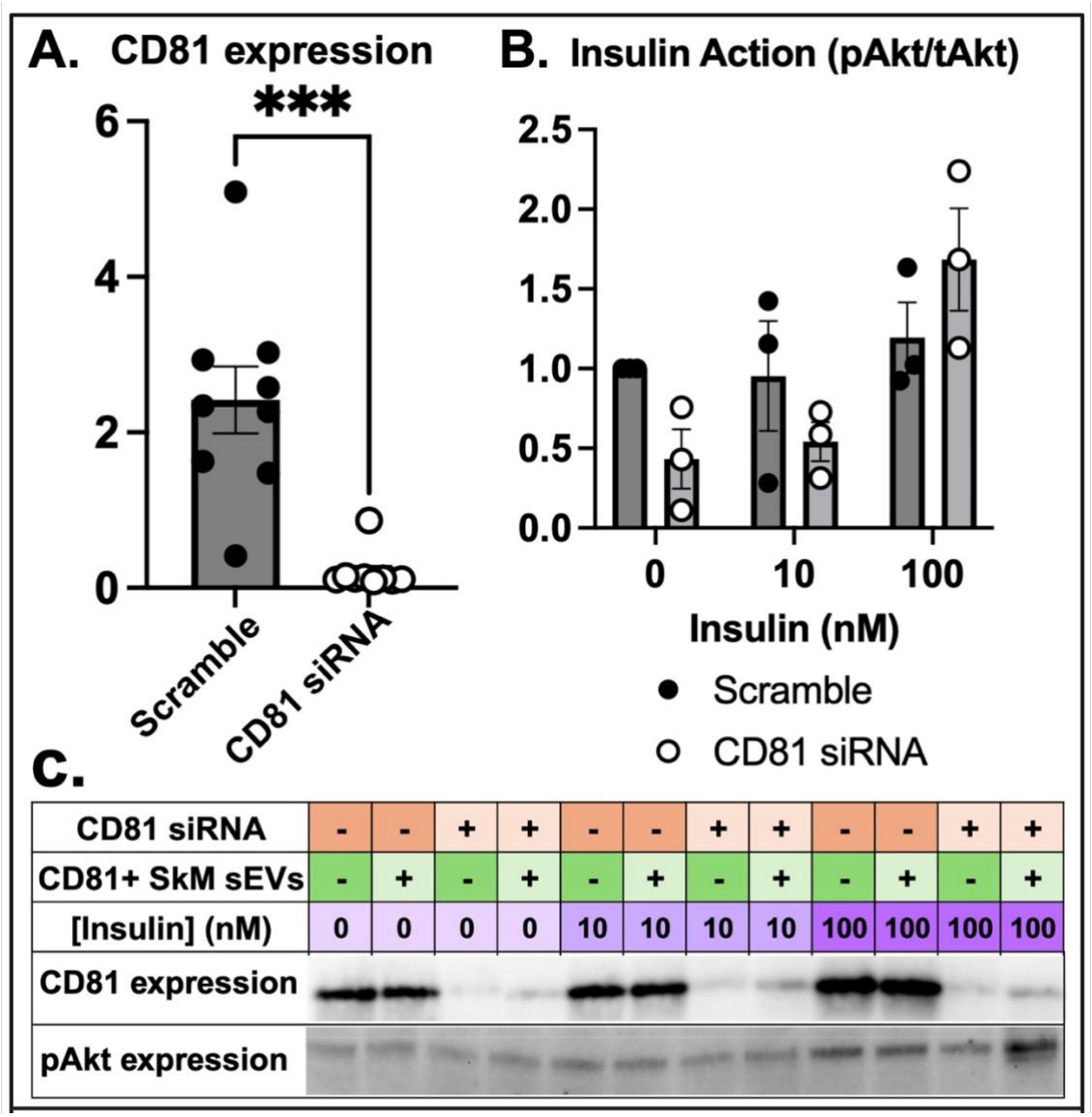

Figure 7: CD81 siRNA treatment significantly decreases CD81 expression in 3T3L1 preadipocytes and may decrease insulin action. (A) CD81 expression in 3T3l1 preadipocytes treated with scramble siRNA vs. CD81 siRNA. (B) Insulin action (pAKT/tAKT) in scramble vs. CD81 siRNA treated 3T3L1 preadipocytes treated with control vehicle (no sEVs) and 0, 10, and 100 nM insulin dose (C) Representative western blot images of all experimental groups probed for CD81 and pAKT. ***p-value < 0.01

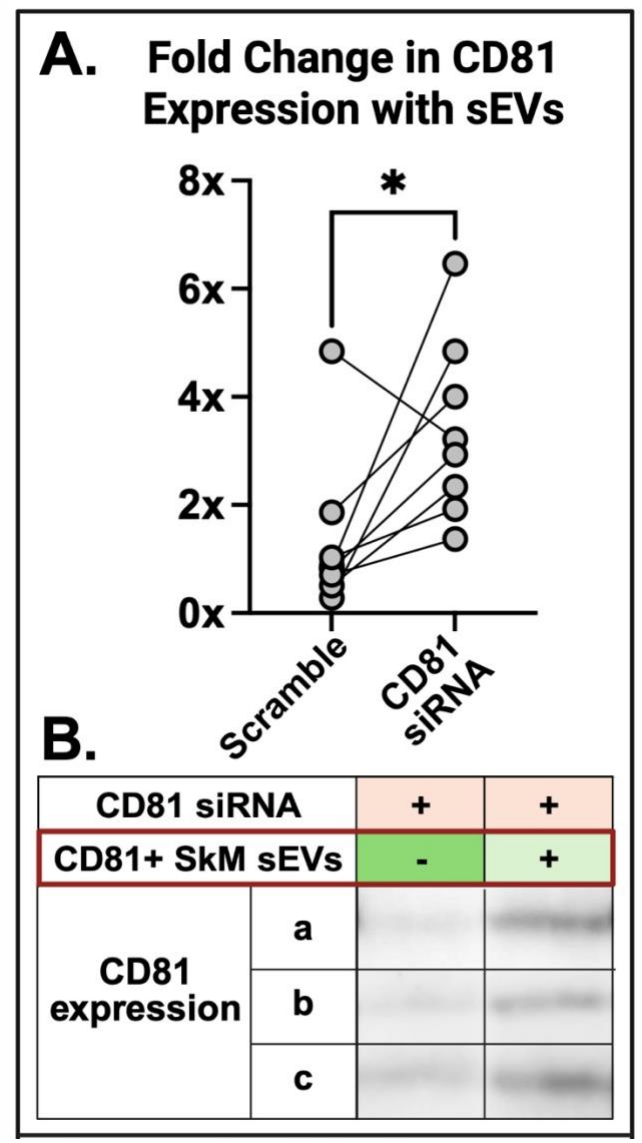

Figure 8: SkM-derived CD81^{+} sEVs increase CD81 expression in CD81-silenced 3T3L1 preadipocytes. (A) CD81 expression fold change in sEV treated 3T3L1 preadipocytes with scramble siRNA vs. CD81 siRNA. (B) Representative western blot images of insulin-stimulated, CD81-silenced 3T3L1 preadipocytes +/- CD81^{+} SkM sEVs probed for CD81. *p-value < 0.05

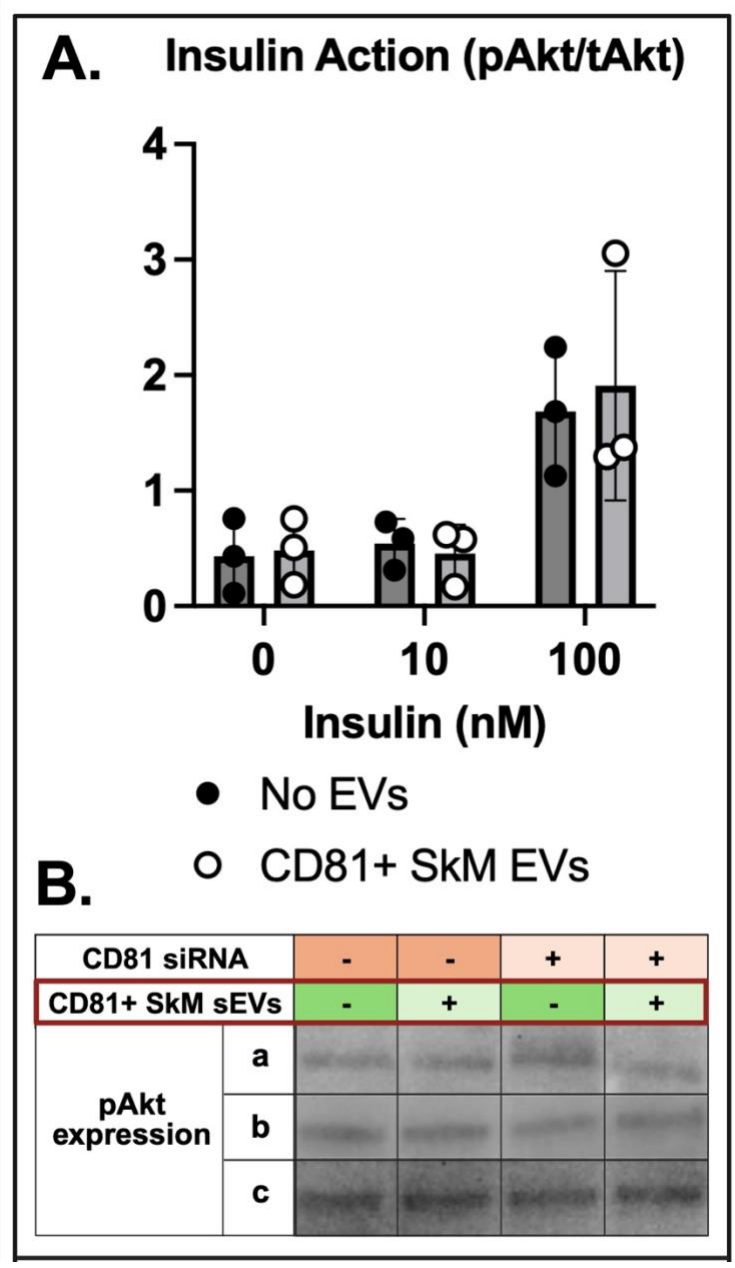

Figure 9:: CD81+ SkM sEVs did not significantly improve insulin action. (A) Insulin action (pAkt/tAkt) of 3T3L1 preadipocytes in the presence vs absence of $CD81^+$ sEVs.(B) Representative western blot images of insulin-stimulated 3T3L1 preadipocyte pAKT expression +/- CD81 siRNA and +/- $CD81^+$ SkM sEVs.

CHAPTER 7 – DISCUSSION AND LIMITATIONS

The purpose of this study was to investigate the role of CD81, a widely expressed membrane-bound tetraspanin and established EV biomarker, in adipocyte insulin signaling. Specifically, we sought to determine how the abundance of CD81 protein either within a cell, or delivered via sEVs, influences insulin action in preadipocytes.

In Aim 1, we demonstrated a physical interaction between CD81 and pAkt in 3T3L1 preadipocytes, as both proteins were detected in the same immunoprecipitated complex under non-denaturing conditions (Figure 6). In Aim 2, we confirmed that CD81-siRNA transfection significantly reduced CD81 expression in preadipocytes (Figure 7A) and observed a modest, though non-significant, trend toward impaired insulin signaling (Figure 7B). In Aim 3, we found that treatment with SkM-derived $CD81^+$ sEVs successfully increased CD81 expression in CD81-silenced 3T3L1 cells (Figure 8A), indicating that EV delivery can restore protein content in a target cell. However, in Aim 4, $CD81^+$ SkM-derived sEV treatment did not significantly improve insulin signaling in preadipocytes (Figure 9A). I discuss the importance of these findings, potential pitfalls and future directions below.

CD81 INTERACTS WITH pAkt BUT NOT TOTAL Akt1 IN PREADIPOCYTES

In Aim 1, we demonstrated a physical association between CD81 and Thr^{308} pAkt, suggesting that CD81 may play a direct role in organizing or stabilizing this isoform of pAkt at the membrane. This interaction suggests that CD81 may facilitate

insulin signaling by recruiting or retaining pAkt in proximity to the insulin receptor complex. This idea is supported by previous literature showing interactions between CD81 and total Akt[66], however, our results are novel in that we detected CD81-pAkt interactions in 3T3L1 preadipocytes. Based on our findings below, the function(s) of CD81-Akt interactions in preadipocytes could to be explored in future studies.

CD81 SILENCING DID NOT SIGNIFICANTLY IMPAIR INSULIN SIGNALING AND CD81$^+$ sEVs DID NOT IMPROVE INSULIN ACTION IN PREADIPOCYTES

Despite successful silencing of CD81 via lipofectamine-siRNA and CD81 protein restoration via SkM-derived CD81$^+$ sEVs, we did not observe significant changes in insulin-stimulated pAkt expression. This contrasts with previous work suggesting that CD81 overexpression enhances Akt-mediated cell migration[66] and loss of CD81 causes IR and adipose tissue dysfunction *in vivo*[13]. There are several possible explanations for our observations. First, compensatory mechanisms may maintain insulin signaling in the absence of CD81 in preadipocytes. The insulin receptor signaling cascade is complex and redundant; adaptor proteins, other scaffolding molecules, or lipid raft integrity may buffer against the impact of partial CD81 depletion, especially given the experimental design employed did not induce physiologically relevant IR. Another explanation involves the method of EV enrichment. The CD81$^+$ sEVs used in this study were isolated via antibody-based magnetic immunocapture, which prioritizes purity of CD81+ sEV populations, an imperative goal of this study. However, this technique may inadvertently impair EV function. The CD81 antibody used in magnetic immunocapture binds to the large extracellular loop (LEL) of CD81, which plays a critical role in CD81's

structural conformation and its ability to organize membrane microdomains[67]. Binding to this region may sterically hinder CD81's capacity to reorganize lipid raft domains or cluster signaling proteins like pAkt and insulin receptors, which could be necessary for its role in insulin action in recipient preadipocytes. Interestingly, the same magnetic bead system was used to immunoprecipitate CD81 in Aim 1, where CD81 and pAkt still co-precipitated. This discrepancy is likely due to anatomical differences in the interaction sites: the magnetic bead-linked antibody binds to the LEL of CD81, while CD81 interacts with pAkt through its intracellular domains. This distinction supports prior literature that the LEL of CD81 is primarily responsible for organizing membrane-associated factors[46,53,67,68], such as the insulin receptor, rather than directly mediating intracellular protein–protein interactions like those with pAKT. This suggests that the bead does not preclude protein–protein interaction altogether, but its impact in the context of dynamic membrane remodeling or signaling initiation in living cells remains uncertain. Together, these data support a structural and signaling role for CD81 at the membrane while also highlighting critical challenges in EV-based therapeutic delivery.

LIMITATIONS

Several limitations within this study should be acknowledged. First, the isolation of sufficient quantities of C2C12-derived sEVs posed a considerable technical challenge. While a total of ~360 mL of conditioned media was collected from C2C12 myotube cultures, the yield of total sEVs remains inherently low in standard *in vitro* systems. This limitation is common in therapeutic EV research, where sourcing cell-type

specific sEVs at sufficient scale for downstream applications continues to hinder translational progress.

Second, all experiments in this study were conducted using undifferentiated 3T3L1 preadipocytes. This choice was made to remain consistent with prior literature, particularly the work of Oguri et al., which identified $CD81^+$ adipocyte progenitor cells as key regulators of insulin sensitivity and adipose tissue remodeling. Moreover, our own preliminary studies were also performed in primary adipocyte progenitor cells, further supporting the use of a progenitor model. However, the use of preadipocytes may have limited the physiological relevance of some findings. Mature adipocytes, with their established lipid storage capacity and increased metabolic demand, may have revealed more pronounced effects of SkM-derived $CD81^+$ sEV treatment on insulin action, particularly through Akt phosphorylation. Furthermore, the use of undifferentiated cells constrained our ability to evaluate functional outcomes related to lipid metabolism, such as lipolysis, fatty acid uptake, triglyceride storage, and non-esterified fatty acid accumulation which would have added depth to the interpretation of CD81's role in adipocyte biology.

Third, as previously discussed, the EV isolation method used to enrich for $CD81^+$ sEVs may have interfered with the functional activity of the captured EVs. Although magnetic immunocapture with CD81-specific antibody-coated microbeads offers high CD81 purity, it involves antibody binding to the large extracellular loop of CD81, a region implicated in protein–protein interactions and membrane organization. The presence of the bead and antibody complex on the CD81 epitope may have sterically

hindered CD81's functional ability to reorganize membrane microdomains or facilitate signaling processes upon EV uptake. While CD81-pAkt interaction was still detectable using this method (as shown in Aim 1), it remains possible that EV-delivered CD81 was not functionally intact, potentially contributing to the lack of observed effects in insulin signaling rescue experiments.

CHAPTER 8 – CONCLUSIONS AND FUTURE DIRECTIONS

This study investigated the role of CD81, a membrane-bound tetraspanin and abundant sEV-associated protein, in adipocyte insulin signaling. We demonstrated that CD81 physically interacts with pAkt in 3T3L1 preadipocytes, supporting its potential involvement in membrane-level coordination of insulin signaling. While CD81 silencing did not significantly impair insulin action in preadipocytes, and exogenous delivery of SkM-derived $CD81^+$ sEVs did not significantly improve preadipocyte insulin sensitivity, $CD81^+$ sEVs successfully increased CD81 protein content in CD81-silenced preadipocytes. These findings suggest that CD81 may play a modulatory role in insulin action, but functional rescue of insulin action may require further optimization of the delivery system or co-delivery of additional signaling molecules.

Several immediate future directions stem from this work. First, future experiments should be repeated in mature adipocytes and compared to our findings here in preadipocytes. Mature adipocytes have a greater metabolic demand for lipid handling, which may reveal more robust or functionally relevant changes in insulin signaling. These experiments should also include quantification of lipid metabolism markers such as non-esterified fatty acids (NEFAs) or glycerol release to assess how $CD81^+$ sEVs influence adipocyte lipolysis and re-esterification pathways. Second, RNA sequencing of SkM-derived $CD81^+$ sEVs could uncover additional molecular cargo delivered to preadipocytes/adipocytes, potentially revealing other molecular modulators of insulin action within SkM-derived $CD81^+$ sEVs. Additionally, improving methods to acquire functional SkM-derived $CD81^+$ sEVs is essential. One alternative approach is to immunocapture sEVs using tetraspanins that co-express with CD81, such as CD9 or

CD63, thereby avoiding antibody blockage of CD81's large extracellular loop (LEL). While this strategy preserves CD81's functional domains, the continued use of magnetic microbeads raises concerns about interference with cellular processes. Thus, future studies should directly evaluate whether magnetic bead presence impairs EV uptake or function in recipient cells. Another promising approach is to treat 3T3L1 adipocytes with size exclusion chromatography (SEC)-isolated sEVs from C2C12 myotubes without immunocapture. Although not CD81-enriched, literature supports robust CD81 expression in SkM EVs[17,18,69]. This strategy may preserve CD81's functionality while enhancing biological relevance. Furthermore, these experiments could be expanded to include C2C12 myotubes subjected to electrical pulse stimulation (EPS) to mimic contractile activity in vitro. Since CD81 expression increases after exercise, comparing the effects of resting vs. "exercised" SkM sEVs on adipocyte insulin signaling could offer new insights into the therapeutic potential of exercise-responsive vesicles.

Together, these next steps will not only deepen our mechanistic understanding of CD81's role in metabolic signaling but also guide the development of EV-based strategies to improve adipocyte insulin sensitivity as a novel therapeutic for obesity and related disease states.

REFERENCES

1. Emmerich, S., Fryar, C., Stierman, B. & Ogden, C. *Obesity and Severe Obesity Prevalence in Adults: United States, August 2021–August 2023*. https://stacks.cdc.gov/view/cdc/159281 (2024) doi:10.15620/cdc/159281.
2. Ward, Z. J. *et al.* Projected U.S. State-Level Prevalence of Adult Obesity and Severe Obesity. *N. Engl. J. Med.* **381**, 2440–2450 (2019).
3. World Health Organization. Obesity.
4. Cross, D. A. E., Alessi, D. R., Cohen, P., Andjelkovich, M. & Hemmings, B. A. Inhibition of glycogen synthase kinase-3 by insulin mediated by protein kinase B. *Nature* **378**, 785–789 (1995).
5. Yang, A. & Mottillo, E. P. Adipocyte lipolysis: from molecular mechanisms of regulation to disease and therapeutics. *Biochem. J.* **477**, 985–1008 (2020).
6. Wu, H. & Ballantyne, C. M. Skeletal muscle inflammation and insulin resistance in obesity. *J. Clin. Invest.* **127**, 43–54 (2017).
7. Kahn, B. B. & Flier, J. S. Obesity and insulin resistance. *J. Clin. Invest.* **106**, 473–481 (2000).
8. Bays, H. E. Adiposopathy. *J. Am. Coll. Cardiol.* **57**, 2461–2473 (2011).
9. Wilding, J. P. H. *et al.* Once-Weekly Semaglutide in Adults with Overweight or Obesity. *N. Engl. J. Med.* **384**, 989–1002 (2021).
10. Yang, X.-P., Lai, D., Zhong, X.-Y., Shen, H.-P. & Huang, Y.-L. Efficacy and safety of canagliflozin in subjects with type 2 diabetes: systematic review and meta-analysis. *Eur. J. Clin. Pharmacol.* **70**, 1149–1158 (2014).

11. Kenny, M. *et al.* Exercise adherence in trials of therapeutic exercise interventions for common musculoskeletal conditions: A scoping review. *Musculoskelet. Sci. Pract.* **65**, 102748 (2023).
12. Kanaley, J. A. *et al.* Exercise/Physical Activity in Individuals with Type 2 Diabetes: A Consensus Statement from the American College of Sports Medicine. *Med. Sci. Sports Exerc.* **54**, 353–368 (2022).
13. Oguri, Y. *et al.* CD81 Controls Beige Fat Progenitor Cell Growth and Energy Balance via FAK Signaling. *Cell* **182**, 563-577.e20 (2020).
14. McIlvenna, L. C. *et al.* Single vesicle analysis reveals the release of tetraspanin positive extracellular vesicles into circulation with high intensity intermittent exercise. *J. Physiol.* **601**, 5093–5106 (2023).
15. Brahmer, A. *et al.* Platelets, endothelial cells and leukocytes contribute to the exercise-triggered release of extracellular vesicles into the circulation. *J. Extracell. Vesicles* **8**, 1615820 (2019).
16. Easterday, D. S. & Lark, D. S. Circulating Tetraspanins: From Markers to Mechanisms Driving Systemic Exercise Adaptation. *Function* **4**, zqad048 (2023).
17. Estrada, A. L. *et al.* Extracellular vesicle secretion is tissue-dependent ex vivo and skeletal muscle myofiber extracellular vesicles reach the circulation in vivo. *Am. J. Physiol.-Cell Physiol.* **322**, C246–C259 (2022).
18. Ismaeel, A. *et al.* Extracellular vesicle distribution and localization in skeletal muscle at rest and following disuse atrophy. *Skelet. Muscle* **13**, 6 (2023).

19. Crewe, C. *et al.* An Endothelial-to-Adipocyte Extracellular Vesicle Axis Governed by Metabolic State. *Cell* **175**, 695-708.e13 (2018).

20. Rana, S., Yue, S., Stadel, D. & Zöller, M. RETRACTED: Toward tailored exosomes: The exosomal tetraspanin web contributes to target cell selection. *Int. J. Biochem. Cell Biol.* **44**, 1574–1584 (2012).

21. Fritzsching, B. *et al.* Release and Intercellular Transfer of Cell Surface CD81 Via Microparticles. *J. Immunol.* **169**, 5531–5537 (2002).

22. Homsi, Y. *et al.* The Extracellular δ-Domain is Essential for the Formation of CD81 Tetraspanin Webs. *Biophys. J.* **107**, 100–113 (2014).

23. Fordjour, F. K. *et al.* Exomap1 mouse: A transgenic model for in vivo studies of exosome biology. *Extracell. Vesicle* **2**, 100030 (2023).

24. Ogden, C. L. *et al.* Trends in Obesity Prevalence by Race and Hispanic Origin-1999-2000 to 2017-2018. *JAMA* **324**, 1208–1210 (2020).

25. About Obesity.

26. Finkelstein, E. A. *et al.* Obesity and severe obesity forecasts through 2030. *Am. J. Prev. Med.* **42**, 563–570 (2012).

27. Vega, G. L., Chandalia, M., Szczepaniak, L. S. & Grundy, S. M. Metabolic correlates of nonalcoholic fatty liver in women and men. *Hepatology* **46**, 716–722 (2007).

28. Saltiel, A. R. & Kahn, C. R. Insulin signalling and the regulation of glucose and lipid metabolism. *Nature* **414**, 799–806 (2001).

29. Sano, H. *et al.* Insulin-stimulated Phosphorylation of a Rab GTPase-activating Protein Regulates GLUT4 Translocation. *J. Biol. Chem.* **278**, 14599–14602 (2003).

30. Anthonsen, M. W., Rönnstrand, L., Wernstedt, C., Degerman, E. & Holm, C. Identification of Novel Phosphorylation Sites in Hormone-sensitive Lipase That Are Phosphorylated in Response to Isoproterenol and Govern Activation Properties in Vitro. *J. Biol. Chem.* **273**, 215–221 (1998).
31. Yamauchi, T. *et al.* Adiponectin stimulates glucose utilization and fatty-acid oxidation by activating AMP-activated protein kinase. *Nat. Med.* **8**, 1288–1295 (2002).
32. Jo, J. *et al.* Hypertrophy and/or Hyperplasia: Dynamics of Adipose Tissue Growth. *PLoS Comput. Biol.* **5**, e1000324 (2009).
33. Hotamisligil, G. S. *et al.* IRS-1-Mediated Inhibition of Insulin Receptor Tyrosine Kinase Activity in TNF-α- and Obesity-Induced Insulin Resistance. *Science* **271**, 665–670 (1996).
34. Houstis, N., Rosen, E. D. & Lander, E. S. Reactive oxygen species have a causal role in multiple forms of insulin resistance. *Nature* **440**, 944–948 (2006).
35. Itani, S. I., Ruderman, N. B., Schmieder, F. & Boden, G. Lipid-Induced Insulin Resistance in Human Muscle Is Associated With Changes in Diacylglycerol, Protein Kinase C, and IκB-α. *Diabetes* **51**, 2005–2011 (2002).
36. Samuel, V. T. *et al.* Mechanism of Hepatic Insulin Resistance in Non-alcoholic Fatty Liver Disease. *J. Biol. Chem.* **279**, 32345–32353 (2004).
37. Perry, R. J., Samuel, V. T., Petersen, K. F. & Shulman, G. I. The role of hepatic lipids in hepatic insulin resistance and type 2 diabetes. *Nature* **510**, 84–91 (2014).
38. Koves, T. R. *et al.* Mitochondrial Overload and Incomplete Fatty Acid Oxidation Contribute to Skeletal Muscle Insulin Resistance. *Cell Metab.* **7**, 45–56 (2008).

39. Xu, H. *et al.* Chronic inflammation in fat plays a crucial role in the development of obesity-related insulin resistance. *J. Clin. Invest.* **112**, 1821–1830 (2003).

40. Khan, T. *et al.* Metabolic Dysregulation and Adipose Tissue Fibrosis: Role of Collagen VI. *Mol. Cell. Biol.* **29**, 1575–1591 (2009).

41. Myers, M. G., Cowley, M. A. & Münzberg, H. Mechanisms of Leptin Action and Leptin Resistance. *Annu. Rev. Physiol.* **70**, 537–556 (2008).

42. Moore, K. J., Sheedy, F. J. & Fisher, E. A. Macrophages in atherosclerosis: a dynamic balance. *Nat. Rev. Immunol.* **13**, 709–721 (2013).

43. Li, H. *et al.* Macrophages, Chronic Inflammation, and Insulin Resistance. *Cells* **11**, 3001 (2022).

44. Wolfe, B. M., Kvach, E. & Eckel, R. H. Treatment of Obesity: Weight Loss and Bariatric Surgery. *Circ. Res.* **118**, 1844–1855 (2016).

45. Seals, D. R., Hagberg, J. M., Hurley, B. F., Ehsani, A. A. & Holloszy, J. O. Effects of endurance training on glucose tolerance and plasma lipid levels in older men and women. *JAMA* **252**, 645–649 (1984).

46. Homsi, Y. *et al.* The extracellular δ-domain is essential for the formation of CD81 tetraspanin webs. *Biophys. J.* **107**, 100–113 (2014).

47. Levy, S., Nguyen, V. Q., Andria, M. L. & Takahashi, S. Structure and membrane topology of TAPA-1. *J. Biol. Chem.* **266**, 14597–14602 (1991).

48. Huang, Y. & Yu, L. Tetraspanin-enriched microdomains: The building blocks of migrasomes. *Cell Insight* **1**, 100003 (2022).

49. Escola, J.-M. *et al.* Selective Enrichment of Tetraspan Proteins on the Internal Vesicles of Multivesicular Endosomes and on Exosomes Secreted by Human B-lymphocytes. *J. Biol. Chem.* **273**, 20121–20127 (1998).

50. Takahashi, S., Doss, C., Levy, S. & Levy, R. TAPA-1, the target of an antiproliferative antibody, is associated on the cell surface with the Leu-13 antigen. *J. Immunol. Baltim. Md 1950* **145**, 2207–2213 (1990).

51. Levy, S., Nguyen, V. Q., Andria, M. L. & Takahashi, S. Structure and membrane topology of TAPA-1. *J. Biol. Chem.* **266**, 14597–14602 (1991).

52. Bradbury, L. E., Kansas, G. S., Levy, S., Evans, R. L. & Tedder, T. F. The CD19/CD21 signal transducing complex of human B lymphocytes includes the target of antiproliferative antibody-1 and Leu-13 molecules. *J. Immunol. Baltim. Md 1950* **149**, 2841–2850 (1992).

53. Serru, V. *et al.* Selective tetraspan-integrin complexes (CD81/alpha4beta1, CD151/alpha3beta1, CD151/alpha6beta1) under conditions disrupting tetraspan interactions. *Biochem. J.* **340 (Pt 1)**, 103–111 (1999).

54. Witherden, D. A., Boismenu, R. & Havran, W. L. CD81 and CD28 costimulate T cells through distinct pathways. *J. Immunol. Baltim. Md 1950* **165**, 1902–1909 (2000).

55. van Zelm, M. C. *et al.* CD81 gene defect in humans disrupts CD19 complex formation and leads to antibody deficiency. *J. Clin. Invest.* **120**, 1265–1274 (2010).

56. Mordica, W. J., Gallagher, R. J., Kennedy, J. L. & Chapes, S. K. Male CD81 knockout genotype disrupts Mendelian distribution of offspring. *Comp. Med.* **60**, 196–199 (2010).

57. Benayas, B. *et al.* Tetraspanin CD81 regulates HSV-1 infection. *Med. Microbiol. Immunol. (Berl.)* **209**, 489–498 (2020).

58. Wu, J. *et al.* Beige adipocytes are a distinct type of thermogenic fat cell in mouse and human. *Cell* **150**, 366–376 (2012).

59. Welsh, J. A. *et al.* Minimal information for studies of extracellular vesicles (MISEV2023): From basic to advanced approaches. *J. Extracell. Vesicles* **13**, e12404 (2024).

60. Lark, D. S., Stemmer, K., Ying, W. & Crewe, C. A brief guide to studying extracellular vesicle function in the context of metabolism. *Nat. Metab.* **6**, 1839–1841 (2024).

61. Pedersen, B. K. & Febbraio, M. A. Muscle as an endocrine organ: focus on muscle-derived interleukin-6. *Physiol. Rev.* **88**, 1379–1406 (2008).

62. Obi, P. O. *et al.* Extracellular Vesicles Released From Skeletal Muscle Post-Chronic Contractile Activity Increase Mitochondrial Biogenesis in Recipient Myoblasts. *J. Extracell. Vesicles* **14**, e70045 (2025).

63. Raposo, G. & Stoorvogel, W. Extracellular vesicles: exosomes, microvesicles, and friends. *J. Cell Biol.* **200**, 373–383 (2013).

64. Merrick, D. *et al.* Identification of a mesenchymal progenitor cell hierarchy in adipose tissue. *Science* **364**, eaav2501 (2019).

65. Vechetti, I. J. *et al.* Mechanical overload-induced muscle-derived extracellular vesicles promote adipose tissue lipolysis. *FASEB J.* **35**, (2021).

66. Martins, S. A., Correia, P. D., Dias, R. A., Da Cruz E Silva, O. A. B. & Vieira, S. I. CD81 Promotes a Migratory Phenotype in Neuronal-Like Cells. *Microsc. Microanal.* **25**, 229–235 (2019).

67. Vogt, S. *et al.* Stabilization of the CD81 Large Extracellular Loop with De Novo Disulfide Bonds Improves Its Amenability for Peptide Grafting. *Pharmaceutics* **10**, 138 (2018).

68. Cunha, E. S. *et al.* Mechanism of Structural Tuning of the Hepatitis C Virus Human Cellular Receptor CD81 Large Extracellular Loop. *Struct. Lond. Engl. 1993* **25**, 53–65 (2017).

69. Whitham, M. *et al.* Extracellular Vesicles Provide a Means for Tissue Crosstalk during Exercise. *Cell Metab.* **27**, 237-251.e4 (2018).

APPENDICES

RAW WESTERN BLOT IMAGES

PLATE A

TOTAL AKT

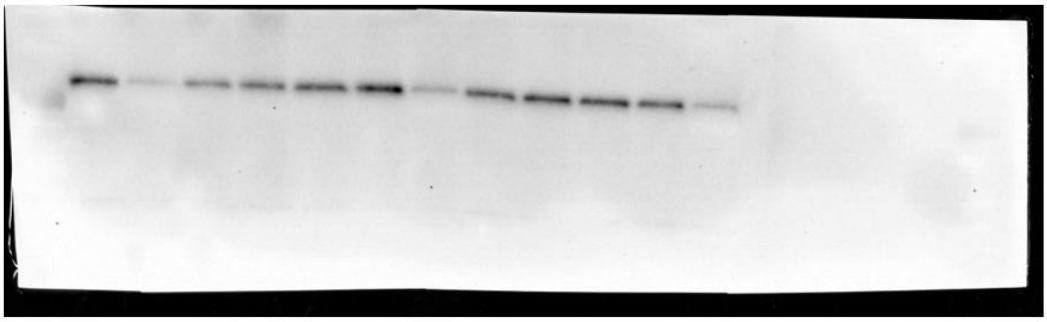

P-AKT

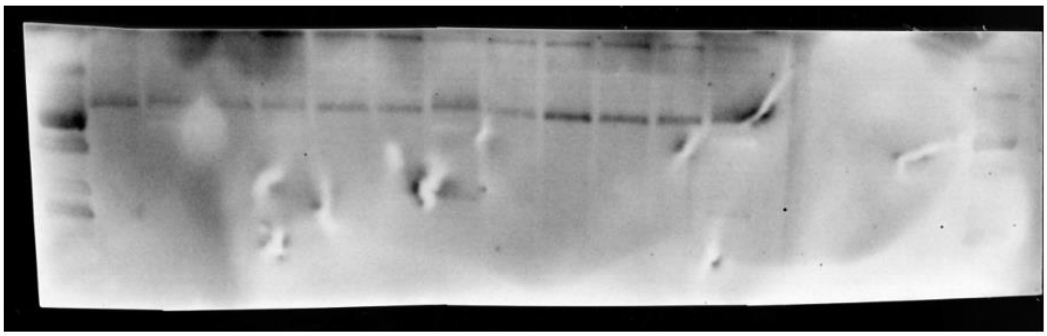

CD81

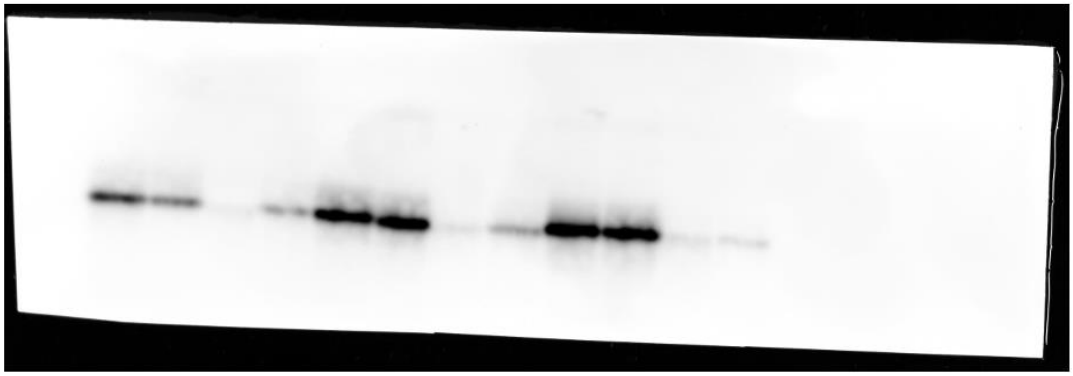

PLATE B

TOTAL AKT

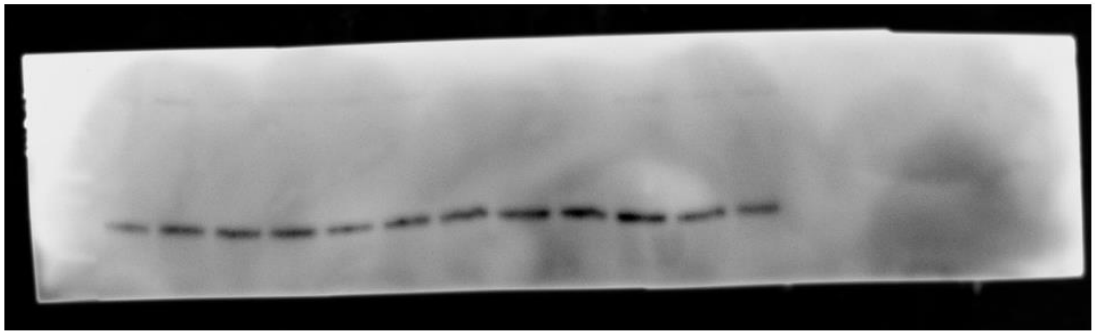

P-AKT

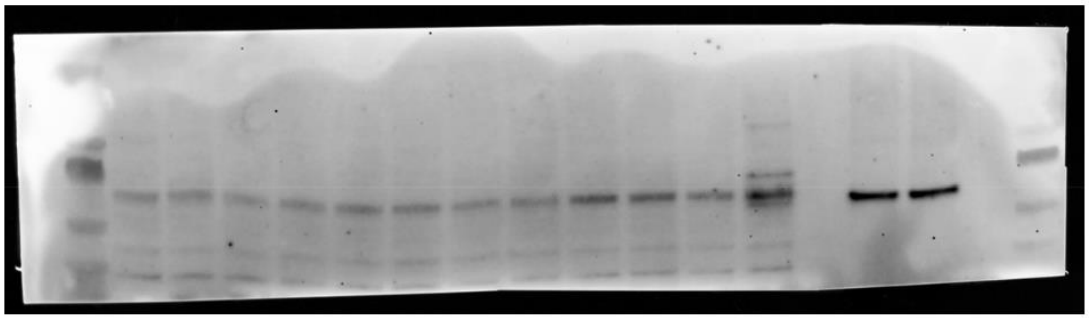

CD81

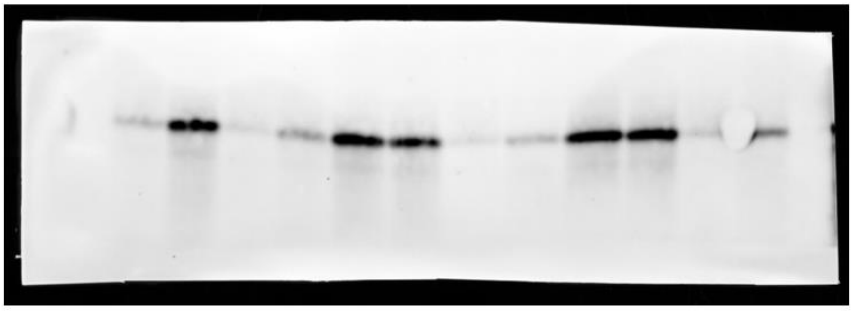

PLATE C

TOTAL AKT

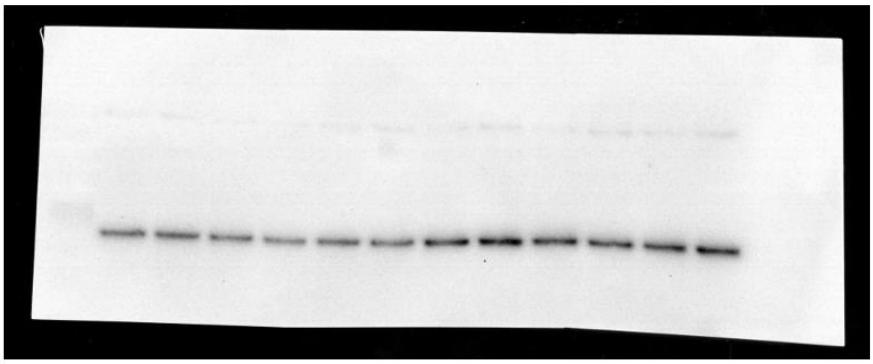

P-AKT

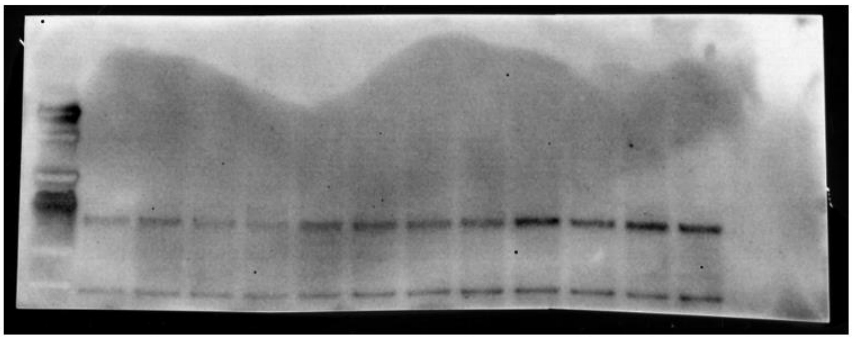

CD81

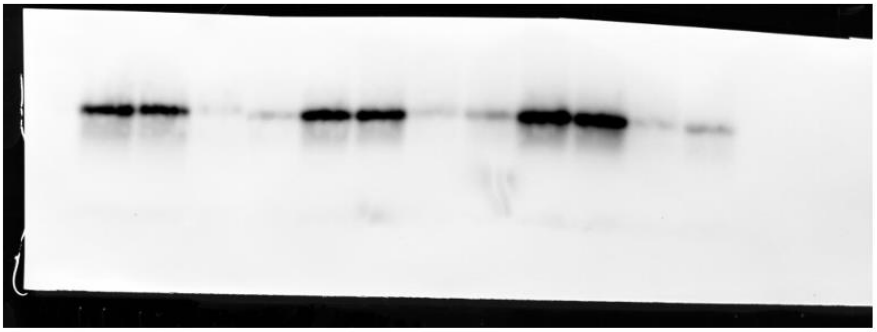

WESTERN BLOT DENSITOMETRY RAW DATA

PLATE A			p-AKT mean	CD81 mean	total AKT mean	p-AKT/AKT	CD81/AKT	AKT ACTIVITY
SCRAMBLE	EVS	0 NM	2096.134	5076.731	2303.548	**0.909958898**	**2.203874632**	1.94689944
SCRAMBLE	EVS	10 NM	3200.296	23718.492	13907.602	**0.230111273**	**1.705433618**	0.492333785
SCRAMBLE	EVS	100 NM	6911.267	28672.463	15303.815	**0.451604192**	**1.873550027**	0.966228199
SIRNA	EVS	0 NM	2628.083	3057.276	8901.137	**0.295252505**	**0.343470278**	0.631706485
SIRNA	EVS	10 NM	2381.205	5386.317	11833.208	**0.201230723**	**0.455186539**	0.430542503
SIRNA	EVS	100 NM	5596.589	1052.92	3211.761	**1.742529721**	**0.327832613**	3.72822349
SCRAMBLE	NO EVS	0 NM	6833.217	13161.572	14619.986	**0.467388751**	**0.900245185**	1
SCRAMBLE	NO EVS	10 NM	4552.075	18065.602	12039.208	**0.378104191**	**1.500563991**	0.808971525
SCRAMBLE	NO EVS	100 NM	12062.673	29697.877	16062.643	**0.750976847**	**1.848878606**	1.606749938
SIRNA	NO EVS	0 NM	1052.335	865.435	6885.409	**0.152835511**	**0.125691154**	0.326998693
SIRNA	NO EVS	10 NM	6604.388	1481.749	2722.933	**2.42546842**	**0.544173874**	5.18940264
SIRNA	NO EVS	100 NM	6164.388	1676.749	11935.451	**0.516477174**	**0.140484763**	1.105026966

PLATE B			p-AKT mean	CD81 mean	total AKT mean	p-AKT/AKT	CD81/AKT	AKT ACTIVITY
SCRAMBLE	EVS	0 NM	4966.761	26767.371	9989.137	**0.497216226**	**2.679648002**	0.676249671
SCRAMBLE	EVS	10 NM	5634.439	19795.057	10544.966	**0.534325004**	**1.87720444**	0.726720266
SCRAMBLE	EVS	100 NM	10378.087	25627.572	15074.38	**0.68845863**	**1.700074696**	0.936353034
SIRNA	EVS	0 NM	3854.033	6108.731	11405.744	**0.337902815**	**0.535583737**	0.459572024
SIRNA	EVS	10 NM	4418.761	3700.69	12272.915	**0.360041685**	**0.301533091**	0.489682473
SIRNA	EVS	100 NM	23418.756	6503.995	9107.38	**2.57140429**	**0.714145561**	3.497293963
SCRAMBLE	NO EVS	0 NM	4721.933	3189.376	6422.167	**0.735255405**	**0.49661991**	1
SCRAMBLE	NO EVS	10 NM	5323.368	27931.492	8116.359	**0.655881289**	**3.441382029**	0.892045518
SCRAMBLE	NO EVS	100 NM	10346.966	26998.179	13882.966	**0.745299383**	**1.944698201**	1.01366053
SIRNA	NO EVS	0 NM	2668.477	1520.335	10105.966	**0.264049671**	**0.150439354**	0.359126461
SIRNA	NO EVS	10 NM	4470.933	1658.335	12840.643	**0.348186068**	**0.129147349**	0.473557985
SIRNA	NO EVS	100 NM	8280.945	2042.82	9356.43	**0.885053915**	**0.218333275**	1.2037367

PLATE C			p-AKT mean	CD81 mean	total AKT mean	p-AKT/AKT	CD81/AKT	AKT ACTIVITY
SCRAMBLE	EVS	0 NM	4935.125	19144.966	13053.522	**0.378068463**	**1.466651376**	0.655586829
SCRAMBLE	EVS	10 NM	6784.045	25085.957	9661.673	**0.702160485**	**2.596440285**	1.217576208
SCRAMBLE	EVS	100 NM	10265.723	44237.768	14274.643	**0.71915795**	**3.099045489**	1.247050537
SIRNA	EVS	0 NM	1745.648	4118.518	8842.602	**0.197413386**	**0.465758608**	0.342323225
SIRNA	EVS	10 NM	5482.903	6463.217	19646.785	**0.279073803**	**0.32897072**	0.483925868
SIRNA	EVS	100 NM	12211.187	4687.246	18359.149	**0.66512816**	**0.255308457**	1.153360578
SCRAMBLE	NO EVS	0 NM	5965.61	20253.966	10344.622	**0.576687094**	**1.95792229**	1
SCRAMBLE	NO EVS	10 NM	4748.054	27351.492	10616.501	**0.447233415**	**2.576318883**	0.775521804
SCRAMBLE	NO EVS	100 NM	11674.48	38464.555	13562.865	**0.860767987**	**2.836019897**	1.492608376
SIRNA	NO EVS	0 NM	2366.134	1865.335	9747.38	**0.24274564**	**0.191367834**	0.420931286
SIRNA	NO EVS	10 NM	7500.167	2252.062	14258.986	**0.525995818**	**0.157939842**	0.912099166
SIRNA	NO EVS	100 NM	11815.602	5561.861	15451.957	**0.764667026**	**0.35994541**	1.325965213

SUPPLEMENTARY FIGURE 1 – SEC ISOLATED C2C12-DERIVED EVS

MANTA INSTRUMENTS
Better Nanoparticle Characterization

REPORT # 202505201304002

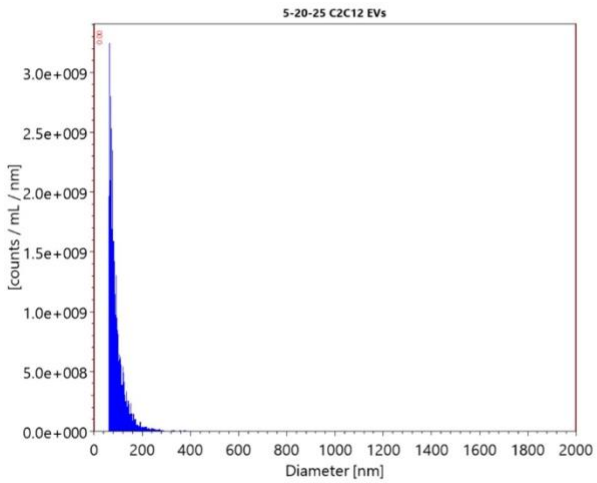

	5-20-25 C2C12 EVs
General	
Date / Time	05/20/2025 / 12:49:09
Measurement type	NTA
Operator / Username	DE / Manta
Measurement authorized by	DL
Measurement location	Fort Collins, CO 80521

Sample	
Sample description	5-20-25 C2C12 EVs
Diluent	Water
Dilution	1250 [times]
Filtering procedure	-

Results	
Total frames / Processed frames	7500 / 7500
Binning	LogBinSilica
Integration range	0 [nm] to 2000 [nm]
Counts within range* / Total tracks*	3337 / 3337
Concentration within range	9.9E+10 [particles/mL]
Diluent concentration within range	1.2E+07 [particles/mL]
Diluent sample name	5-20-25 dil1
Concentration without diluent	8.4E+10 [particles/mL]
Average size within range	94 [nm]
Standard deviation of size / CV	43 [nm] / 0.45 CV
Modal size	64 [nm]
D10 / D50 / D90*	7.9 [nm] / 57 [nm] / 142 [nm]
Average viscosity	0.95 [cP]

*computed with ConstantBins table